VI Session: RADAR OBSERVATIONS OF THE MOON

Radar Studies of the Moon

J. V. Evans

Lincoln Laboratory[1], Massachusetts Institute of Technology, Lexington, Mass.

Accurate range measurements have been reported only by the group working at the Naval Research Laboratory. Their most recent value for the mean center-to-center distance between the Earth and the Moon is 384,400.2 ± 1.1 km and is based upon a value for the Earth's radius of 6,378,170 m which seemed most consistent with the observed diurnal variation in range.

The absolute cross section of the Moon has been determined over a wide range of wavelengths to a precision in most cases of ± 3 dB. Unfortunately, this uncertainty is too large to permit any definite conclusions to be drawn concerning the wavelength dependence in the cross section. The observations suggest that the cross section remains constant at about 7 percent of the projected area of the Moon's disk at wavelengths in the range 1 cm to 1 m, and perhaps rises to 10 percent or higher at wavelengths in the range 1 to 10 m.

Short-pulse observations can be used to explore the angular dependence in the scattering of radio waves by the lunar surface. Useful measurements have been made at wavelengths of 1130, 68, 23, 10, and 3.6 cm. The angular dependence has also been investigated at 8.6 mm, though here the angular resolution afforded by a narrow pencil-beam antenna was employed. At all six wavelengths, it appears that part of the echo arises from a highlight located at the center of the Moon's visible disk. A second component comes almost equally from the remaining parts of the surface. The division of power in the two components changes markedly as the wavelength is reduced. At 68-cm wavelength, 80 percent of the power is returned from the highlight, but at 8.6 mm only 15 percent can be associated with this component. The angular power spectrum observed for the power from the highlight also changes with wavelength, indicating that the rms slope of the surface increases as the wavelength is reduced. These observations have been interpreted as indicating that there is a wide range of structure sizes on the Moon.

The deduced values of dielectric constant range from $k = 2.79$ down to $k = 2.13$. In view of the greater experimental difficulties together with the doubtful validity of the assumptions at 8.6-mm wavelength, this apparent wavelength dependence should be accepted with caution. If real, it may be caused by the finite conductivity of the material (i.e., $s \neq 0$ in (6)) or by inhomogeneity in the surface layers—the density perhaps increasing slightly with depth. These values certainly indicate that the surface is broken or porous in texture—the material occupying perhaps about 30 percent of the available volume. In short, the echo intensity and angular spectrum is comparable to that observed from aircraft over terrestrial deserts.

1. Introduction

The smallest objects on the lunar surface that are resolvable by means of large ground-based optical telescopes have dimensions of the order of 1/2 km. At the other extreme, photometric studies [Hapke and Van Horn, 1963] and polarization measurements [Dollfus, 1962] yield information about the microstructure which may at most be measured in millimeters. The success of manned exploration of the lunar surface may depend to a large extent upon the nature of the surface in the range of sizes between these two extremes. If the surface were densely covered with craters below the optical limit of resolution, or for that matter boulders of a size comparable with a landing vehicle, severe difficulties would be encountered. Until close-proximity photographs were obtained, one could be guided only by radar results. These suggested that the surface is not necessarily very hostile—a result that has partly been confirmed by the Ranger pictures. The existence of the Moon as a target against which both equipment and theoretical ideas may be tested should prove very valuable in obtaining and understanding the reflected signals from Venus, Mercury, and Mars.

A historical review of the early radar observations of the Moon has been given by Evans [1962a], and here we shall present only what seems the best available experimental evidence concerning the Moon's scattering behavior. For the most part, this has been obtained by measuring the distribution of the echo power as a function of range delay using short-pulse transmissions. Additional measurements in which both the range and Doppler resolution of the radar are exploited have shown that, though the larger part of the Moon's surface is rather featureless to radar observation, the newer (rayed) craters are extraordinarily bright with respect to their surroundings. The experimental observations described here have stimulated a large number of theoretical workers to attempt to deduce from the scattering properties of the Moon a physical description of its surface. There is as yet no complete understanding of the scattering behavior of a surface which contains structure of sizes both larger and smaller than the wavelength. As a result, the success with which the radar results have been interpreted remains limited. Here we shall review only the approaches that seem to offer the most promise of success.

[1] Operated with support from the U.S. Air Force.

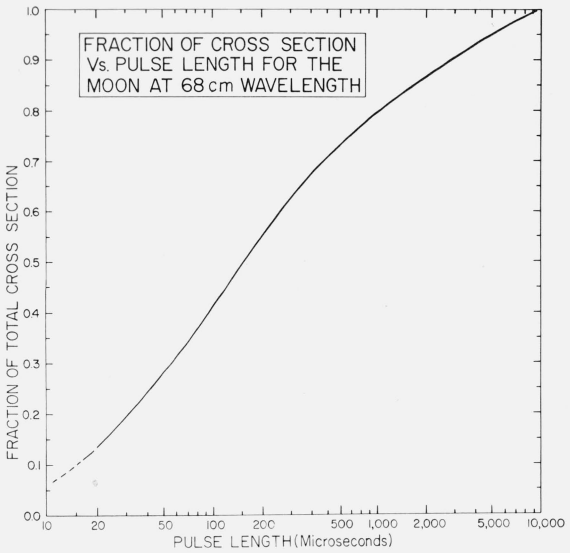

FIGURE 1. *The peak cross section of the moon expressed as a percentage of the total cross section σ plotted as a function of pulse length.*

The radar depth of the moon is 11.6 msec, and if pulses shorter than this are employed, the echo power will fall due to the reduction in the instantaneous area illuminated by the pulse. This curve has been obtained from measurements at 68 cm.

2. Echo Power

2.1. The Radar Equation for a Distributed Target

The radar equation is normally stated in a manner that is proper for the observation of "point targets," i.e., objects which when viewed from the radar subtend an angular diameter much smaller than that of the antenna beam. In this case the received echo power P_r may be stated as

$$P_r = \frac{P_t G A \sigma}{(4\pi R^2)^2} \text{ watts} \tag{1}$$

where P_t = transmitted power (watts), G = antenna gain, A = antenna aperture (m^2), σ the cross section of the target (m^2), and R is the target's range (m). Of all the celestial objects detectable by means of radar, the Moon (and perhaps the Sun) are the only ones in which the target angular diameter is likely to be as large or larger than the antenna beam. The cross section σ observed during observations of the Moon depends, therefore, upon the distribution of the incident power over the surface. In practice, the Moon reflects preferentially from regions near the center of the disk and little loss in total reflected power will be observed until the antenna beamwidth (between half-power points) is made smaller than the angular extent of the Moon (1/2°). Thus for most forms of simple antennas this effect will not be important until the antenna diameter becomes larger than 100 λ where λ is the radio wavelength.

Radar echoes from any of the nearby objects in the solar system can, however, be resolved in range delay or in frequency. For example, it is readily possible to transmit pulses which are of insufficient length to illuminate the whole of a planet's visible hemisphere. In the case of the Moon, a pulse of 11.6 msec is required to fully illuminate the surface, and if shorter pulses are employed, the effective or instantaneous cross section σ will never reach its maximum possible value (the CW cross section). Figure 1 shows how the peak instantaneous cross section falls as a function of pulse length for observations of the Moon at 68-cm wavelength. Because the largest part of the power is reflected from the nearest regions of the lunar surface, an appreciable reduction in cross section is not observed until pulses shorter than 1 msec duration are used. Figure 1 is applicable only for wavelengths of about 50 cm, or longer, as the scattering properties of the surface change markedly toward shorter wavelengths. Equally, where a CW radar is employed, the apparent rotation of the Moon may cause the reflected signals to be appreciably Doppler-broadened. If the receiver employs a narrowband filter which does not accept all the frequency components of the reflected signal, then again the observed cross section will be lower than the full value.

In this review we shall use the term σ to denote the total cross section of the Moon. This could be measured with a radar employing an antenna beam of 1/2° or more by determining the peak echo power observed when pulses of 11.6 msec or longer are transmitted. In practice, echoes from the Moon are found to fade as a consequence of constructive and destructive interference between signals arriving from different parts of the lunar surface. Thus, an average value for the peak echo power (or mean square of the echo amplitude) must be obtained from many pulses to determine σ reliably. Alternatively, with a CW radar, many independent determinations of the echo power are required. In some of the earliest radar observations of the Moon [e.g., DeWitt and Stodola, 1949] this was not recognized and only the maximum value of the echo intensity was reported.

When the antenna beam width is comparable with the diameter of the Moon, it is possible to compute σ if the distribution of incident power over the surface is known (defined by the antenna pattern) and the brightness distribution observed for the lunar disk for uniform illumination is also known. Thus, if the axis of the antenna beam is directed at the center of the Moon, and the antenna pattern is circularly symmetrical about this axis, the echo power is given by

$$P_r = \frac{P_t G_0^2 \lambda^2 \sigma}{64\pi^3 R^4} \int_\theta F^2(\theta) B(\theta) 2\pi \sin\theta d\theta, \tag{2}$$

in which G_0 is the gain of the antenna on axis and λ is the radio wavelength. Here θ is the angle subtended at the radar between the beam axis and an annulus of width $d\theta$ on the lunar surface, $F(\theta)$ is the normalized antenna pattern (power versus angle, $F(\theta)=1$ for $\theta=0°$), and $B(\theta)$ is the distribution of surface brightness that would be observed for uniform illumination; $B(\theta)$ is normalized so that the integral in (2) tends to unity for broadbeam antennas. The term $F(\theta)$ ap-

pears as a square term, as the antenna weights the transmission and reception equally.

Where the antenna beam is broad but the pulse length τ is shorter than the radar depth of the Moon, the echo power is given in

$$P_r = \frac{P_t G A \sigma}{(4\pi R^2)^2} \int_0^{\tau} P(t)dt, \tag{3}$$

where $P(t)$ is the distribution of echo power with delay t (relative to the leading edge of the Moon) measured with a short pulse τ' as $\tau' \to 0$ (it is sufficient for $\tau' << \tau$). The integral in (3) becomes unity for $\tau \geq 11.6$ msec. The general case where the antenna beam is smaller than the diameter of the Moon and short pulses are employed has been treated [Evans, 1962b] by graphically integrating areas inside contours of equal incident energy and equal range. By repeating the observations for different positions of the antenna beam with respect to the Moon's center, it was possible to recover $P(t)$ and thence σ.

2.2. Range Variation

The mean range of the Moon is 3.844×10^8 m (causing an echo delay of 2.56 sec) but due to the ellipticity of the Moon's orbit, the actual range may vary over ± 8 percent of the mean range. As a result, the echo power will vary over a lunation by ± 30 percent (about ± 1 dB). The accuracy achieved in most radar experiments is insufficient for this to be detected, and Fricker et al., [1958] appear to be the only workers who have observed this variation of echo power during the month. Even they were unable to observe this small variation (about 0.2 dB) introduced by the rotation of the Earth. These range changes are easily detected by measuring the echo delay time. Very accurate measurements have been made by Yaplee et al., [1958, 1959, 1964] from which a mean center-to-center distance between the Earth and the Moon of $384{,}400.2 \pm 1.1$ km has been obtained.

The difference between the echo power expected on a given day and the mean echo power is given by

$$\Delta P_r = 40\ [\mathrm{Log}_{10}\ \pi - 1.756]\ \mathrm{dB}, \tag{4}$$

where π is the daily value of the equatorial horizontal parallax tabulated in the Nautical Almanac and American Ephemeris in minutes of arc.

2.3. Observed Values of Cross Section

Many observers have reported values of σ and some of these are presented in table 1 and plotted in figure 2. The values have been presented as fractions of the physical cross section of the Moon ($\pi a^2 = 9.49 \times 10^{12} \mathrm{m}^2$), and span a range of over 10 octaves (from 8.6 mm to 22 m). The increase in cross section with increasing wavelength suggested by figure 2 depends largely on the three long-wave measurements reported by Davis and Rohlfs [1964]. These measurements may have been subject to systematic errors introduced by ionospheric effects. If these three points are ignored the remainder show no clear wavelength dependence. In part this is caused by the large error bars associated with each measurement which may conceal a marked dependence. The errors given in table 1 are the reported values where these have been given, or ± 3 dB where no uncertainty was published. Absolute power measurements appear to be more difficult in radar astronomy observations than radio astronomy for several reasons. In the first place, the uncertainty in the antenna performance (typically ± 1 dB) enters twice. Next there is the uncertainty associated with measuring P_t; and finally, errors arise in the measurement of P_r due in part to the fading of the signals.

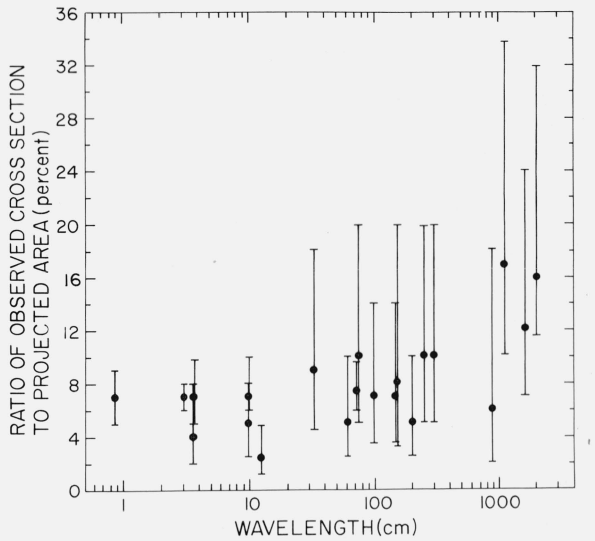

FIGURE 2. *The variation of the total cross section σ as a function of the radar wavelength λ.*

These values are expressed as a fraction of the moon's projected disk πa^2 and have been obtained from the papers listed in table 1.

TABLE 1. *Values for the radar cross section of the Moon as a function of wavelength reported by various workers*

Author	Year	Wavelength	$\sigma/\pi a^2$	Estimated error
		cm		*dB*
Lynn et al.	1963	0.86	0.07	±1.
Kobrin	1963*	3.0	.07	±1.
Morrow et al.	1963*	3.6	.07	±1.5
Evans and Pettengill	1963a	3.6	.04	±3.
Kobrin	1963*	10.0	.07	±1.
Hughes	1963*	10.0	.05	±3.
Victor et al.	1961	12.5	.022	±3.
Aarons	1959**	33.5	.09	±3.
Blevis and Chapman	1960	61.0	.05	±3.
Fricker et al.	1960	73.0	.074	±1.
Leadabrand	1959**	75.0	.10	±3.
Trexler	1958	100.0	.07	±4.
Aarons	1959**	149.0	.07	±3.
Trexler	1958	150.0	.08	±4.
Webb	1959**	199.0	.05	±3.
Evans	1957	250.0	.10	±3.
Evans et al.	1959	300.0	.10	±3.
Evans and Ingalls	1962	784.0	.06	±5.
Davis and Rohlfs	1964	1130.0	.19	+3. −2.
Davis and Rohlfs	1964	1560.0	.13	+3. −2.
Davis and Rohlfs	1964	1920.0	.16	+3. −2.

*Revised value [private communication; Evans and Pettengill, 1963a].
**Reported by Senior and Siegel [1959, 1960].

Unless extraordinary care is taken, the uncertainty in absolute intensity is usually of the order of ± 3 dB. That Fricker et al., [1958] are the only observers who have reported observations of the monthly variation of P_r (which is 2 dB) is indicative of the difficulties encountered. Even in the case of Fricker's results, it was not possible to determine the absolute value of σ to better than ± 1 dB. Because the Moon is an extended target whose characteristics change with wavelength, it does not serve radar astronomers as a reference in the manner that certain radio sources (e.g., Cygnus A) are used by radio astronomers. Radar astronomy would benefit by the launching of a spherical reflector into a near synchronous orbit which could become a standard test target. Any wavelength dependence in the lunar cross section would then be obtainable with greater confidence. The mean of the values listed in table 1 is close to 0.07, and using this mean value, the term $\frac{\sigma}{(4\pi R^2)^2}$ has a value of about 1.95×10^{-25} m^{-2}. This term represents the "path loss" encountered by a signal transmitted by an antenna of unit gain and received by one of unit aperture. Expressed in this fashion, the path loss is independent of wavelength and may be taken as 247.2 dB/m^2.

2.4. Theoretical Values of the Cross Section

If the Moon were a perfect sphere having a power reflection coefficient at normal incidence of ρ_0, then the cross section would be [Senior and Siegel, 1959]

$$\sigma = \rho_0 \pi a^2, \tag{5}$$

it being assumed that $a >> \lambda$. The Fresnel reflection coefficient ρ_0 is related to the electrical constants of the surface by $\rho_0 = |Q|^2$ where

$$Q = \frac{1 - \sqrt{\left[\frac{\mu_0}{\mu}\left(\frac{\epsilon}{\epsilon_0} + i\frac{s}{\omega\epsilon_0}\right)\right]}}{1 + \sqrt{\left[\frac{\mu_0}{\mu}\left(\frac{\epsilon}{\epsilon_0} + i\frac{s}{\omega\epsilon_0}\right)\right]}}. \tag{6}$$

Here ϵ = permittivity, μ = permeability, and s = conductivity (the subscript 0 denotes free-space values), and ω is the angular radiowave frequency. It can be seen that $\rho_0 (= |Q|^2)$ will depend upon the wavelength, unless s, the conductivity, is zero or infinite. In the case of a perfect dielectric where $\mu \rightarrow \mu_0$ and $s \rightarrow 0$, (6) simplifies to

$$Q = \frac{1 - \sqrt{k}}{1 + \sqrt{k}}, \tag{7}$$

where $k = \epsilon/\epsilon_0$ is the relative dielectric constant. Values of k for some typical rock mineral samples are given in table 2. These have been taken from many values listed in a report by Brunschwig et al., [1960]. The selection in table 2 is somewhat arbitrary,

TABLE 2. *Some typical terrestrial rocks and their values of dielectric constant [Brunschwig et al., 1960]*

Mineral	Type	Source	Dielectric constant k
Andesite	Vesicular basalt	Chaffee County, Colo.	6.51
Olivine basalt, cellular		Washington	5.50
Basalt	Olivine basalt	Jefferson County, Colo	8.89
Olivine basalt	Basalt	Lintz, Rhenish Prussia	17.4
Diabase		Mt. Tom, Mass	10.8
Rhyolitic pumice	Pumice	Millard County, Utah	2.29
Rhyolite		Castle Rock, Colo	4.00
Basaltic scoria	Scoria	nr. Klamath Falls, Oreg	6.08
Trachytic tuff		nr. Cripple Creek, Colo	5.32
Quartz sandstone	Sandstone	Columbia County, Pa	4.84

but does indicate the wide scatter of values encountered. The basaltic specimens examined by Brunschwig et al., [1960] showed the greatest range of values (from 5.5 to 26.7) and an average value for the seven samples listed is 14. For the minerals listed as forms of andesite (5 samples) the mean was 8.8, while the rhyolitic samples were lower (4.1). Silicate materials, e.g., fused quartz, are frequently suggested as making up the bulk of the lunar surface material and these have dielectric constants in the range 4 to 7.[2] Dry terrestrial sand has a dielectric constant of about half this. If the surface of the Moon were solid rock having a dielectric constant $k = 5$ (the lowest value likely), then the reflection coefficient would be 14 percent. As the mean lunar cross section is only 7 percent, it is already evident that the surface cannot be solid rock.

If the perfect sphere discussed above is replaced by one in which the true surface departs in an irregular fashion from the mean, then the cross section is likely to change and account can be taken of this by writing

$$\sigma = g\rho_0 \pi a^2. \tag{8}$$

Here g is a directivity factor that expresses the ability of the sphere to scatter back favorably toward the source. For a smooth metal sphere ($\rho_0 = 1$) the echo power is reradiated isotropically and the value of g is 1.0 [Norton and Omberg, 1947]. As we have seen, the factor g is also unity in the case of a smooth dielectric sphere, but the scattering in this case is not isotropic and depends upon the dielectric constant k [Rea, Hetherington, and Mifflin, 1964].

The value for g as defined by (8) for an arbitrarily rough surface is not known and only the case of a sphere with a smooth undulating surface has been examined in detail [Hagfors, 1964]. In this case $g = 1 + \alpha^2$ where α^2 is half the mean square surface slope. The effect of the shallow undulations is to cause the pattern of Fresnel zones at the center of the disk to be rearranged such that parts of each zone are distributed randomly over the entire disk. Provided that the antenna beam is broad enough to illuminate the whole surface, a small increase in mean

[2] An alternative argument due to Gold [1964] is to suppose that fractionation processes have not occurred in lunar rocks to the extent they have on Earth. The surface rocks would then be expected to be little different from meteoritic material and have a high dielectric constant ($k \sim 20$).

cross section will be observed when this hypothetical ideally smooth sphere is replaced by one with an undulating surface.

An alternate and widely adopted approach to obtaining the scattering cross section is to consider the scattering properties of the target as specified by a function $\sigma_0(i\phi\theta)$ which defines the reflected intensity per unit surface area per steradian. This function is obtained by exploring the power reflected from an elemental area of surface illuminated at an angle of incidence i, and observed at an angle of reflection ϕ; the planes containing these two rays and the surface normal are at an angle θ as shown in figure 3. Provided there is no coherence between returns from different surface elements, the gain G_m of the Moon in the direction of backscattering is given by [Evans and Pettingill, 1963b]

$$G_m = \frac{4\pi \int_0^{\pi/2} \sigma_0(i) \sin i \, di}{\int_0^{\pi/2} \int_0^{\pi/2} \int_0^{2\pi} \sigma_0(i\phi\theta) \sin i \sin \phi \, d\theta d\phi di}, \quad (9)$$

where $\sigma_0(i)$ is the particular case in which $i=\phi$, $\theta=0$. From Earth-based observations alone only $\sigma_0(i)$ can be determined and hence G_m as defined by (9) cannot be obtained. If, however, G_m were known either from theory or observation, the cross section for the whole sphere could be written as

$$\sigma = G_m \bar{\rho} \pi a^2. \quad (10)$$

Here $\bar{\rho}$ is the albedo averaged over the hemisphere, and this is usually different from the reflection coefficient at normal incidence ρ_0. This distinction has not always been recognized and the literature contains several instances where ρ_0 has been equated with $\bar{\rho}$ without proper explanation. If this is done, the directivity factor g is automatically made the same as G_m. Rea, Hetherington, and Mifflin [1964] have pointed out that these approximations are certainly not valid for the case of a smooth dielectric sphere.

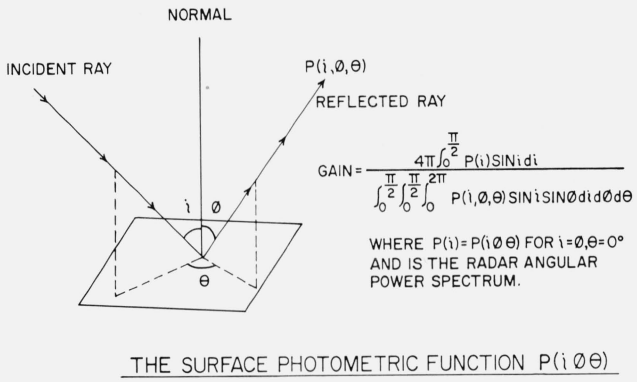

FIGURE 3. *The geometry required for studying the complete scattering characteristics of an irregular surface in order to obtain a value for the gain of the whole moon over an isotropic scatterer.*

3. Echo Power Versus Delay

3.1. Relation to the Angle of Incidence

With modern radar equipment, echoes from the Moon may readily be resolved either in delay or in frequency. The libration of the Moon causes the lunar disk to appear to be rotating to a terrestrial observer with a radial velocity usually in the range 10^{-6} to 10^{-7} rad/sec. This gives rise to Doppler broadening of the signals so that the echo power at a given frequency offset is proportional to the reflectivity of a particular strip on the Moon's disk that is parallel to the apparent axis of rotation as shown in figure 4 [Browne et al., 1956]. Thus the determination of the echo power spectrum $\bar{P}(f)$ yields the brightness distribution over the Moon's disk. Such measurements have been made by a number of workers [Evans, 1957; Evans and Ingalls, 1962; Daniels, 1963a]. The best measurements of this kind have been performed using phase coherent radar systems, such as the Millstone Hill radar which was employed by Pettengill and Henry [1962a] to obtain the results shown in figure 5. The limb-to-limb Doppler broadening introduced by the Moon is typically 2 c/s for a radar frequency of 100 Mc/s, and hence it is difficult to achieve good

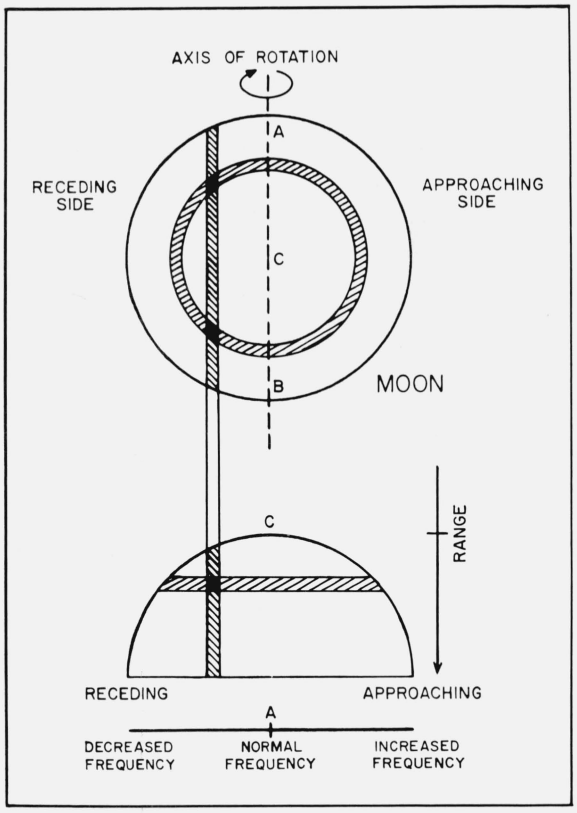

FIGURE 4. *The contours of constant delay* t *and constant Doppler shift* f *are shown for a hypothetical pair of values.*
The shaded regions indicate the two areas having the same frequency and range coordinates.

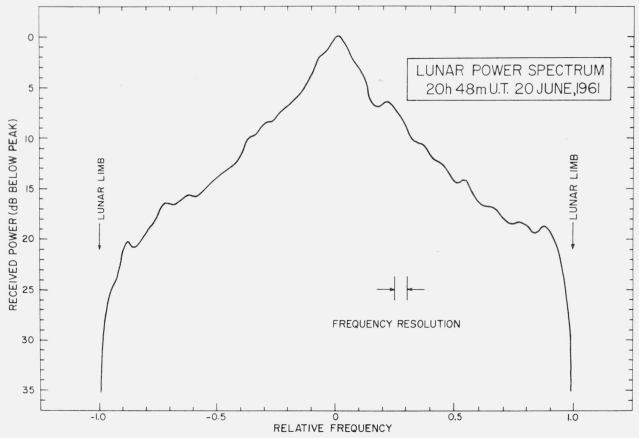

FIGURE 5. *The power spectrum* $\bar{P}(f)$ *of moon echoes obtained by Fourier analyzing a chain of coherent pulses by means of a fast digital computer.*
These observations were made at 68-cm wavelength and show the brightness distribution across the lunar disk.

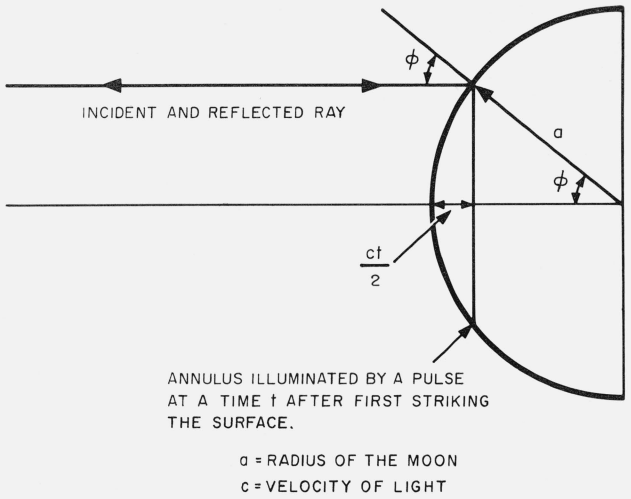

FIGURE 6. *The relation between the range delay* t *and the angle of incidence and reflection* ϕ *of the radio waves.*

resolution by this technique. In figure 5, for example, the frequency resolution of the radar is 1/40th of the total echo spectrum.

Much better resolution can be obtained by resolving the echoes with respect to delay. For example, pulse lengths of 12 μsec and shorter have been used to study the scattering behavior of the Moon (whose full radar depth is 11.6 msec). A short pulse illuminates at any instant an annulus on the surface as shown in figure 4. The amount of *actual* area illuminated by the pulse is given by $\pi ac\tau$ (where c = the velocity of light and τ is the pulse length) and is independent of delay t. However, the *projected* area will vary with the cosine of the angle of incidence ϕ where

$$\phi = \cos^{-1}(1 - ct/2a). \tag{11}$$

Thus if the Moon behaved as a uniformly bright reflector (as it does optically), the average echo power versus delay function $\bar{P}(t)$ would have the form

$$\bar{P}(t) \propto 1 - \frac{ct}{2a}. \tag{12}$$

Herein lies a second advantage of short pulse measurements; namely, there is a singular relation between the angle of incidence ϕ and the delay t [specified by (11)] as shown in figure 6. It follows that by determining the echo power as a function of delay $\bar{P}(t)$, one can determine directly the angular power spectrum $\bar{P}(\phi)$ of the echoes. We choose a function $\bar{P}(\phi)$ of the same form as the function $\sigma_0(i\phi\theta)$ used in (9), i.e., normalized to unit *actual* surface area. It follows that for a uniformly bright surface we have from (12)

$$\bar{P}(\phi) \propto \cos\phi \qquad \text{(Lommel-Seeliger)}, \tag{13}$$

and for Lambert's law

$$\bar{P}(\phi) \propto \cos^2\phi \qquad \text{(Lambert)}. \tag{14}$$

In all likelihood, the surface of the Moon may be regarded as statistically uniform from annulus to annulus. It follows that by exploring the distribution of echo power with delay $\bar{P}(t)$, one can see if the angular power spectrum can be represented by simple laws such as (13) or (14). That is, if the surface is statistically uniform, then the plot $\bar{P}(\phi)$ obtained is simply the angular scattering law $\sigma_0(\phi)$ defined previously. To make it clear that an assumption is involved here, we shall use the symbol $\bar{P}(\phi)$ to denote the angular dependence obtained from short pulse measurements. In the limit, where very short pulses (i.e., as $\tau \to 0$) are used to observe a statistically uniform sphere, $P(\phi) \to \sigma_0(\phi)$.

3.2. Short-Pulse Observations

Kerr and Shain [1951] were the first to attempt short-pulse observations of the Moon in order to see if the pulses were lengthened by the distribution of the scattering centers in depth. They reported that 1-msec pulses were lengthened in support of their conclusion (obtained from echo spectrum measurements) that the Moon was approximately a uniformly bright reflector. Evans [1957] using 2-msec pulses reached the reverse conclusion in support of his observation (also from echo spectrum measurements) that the Moon was in fact a limb dark scatterer. Immediately on publication of these later results, the work performed several years previously at the Naval Research Laboratory was released [Trexler, 1958]. Trexler employed a radar operating at 198 Mc/s with pulse length of 12 μsec and figure 7 illustrates the range display observed in this work. Some 50 percent of the echo power was returned within the first 50 μsec of the pulse. The exponential tail of the echo appeared to extend some 500 μsec beyond the leading

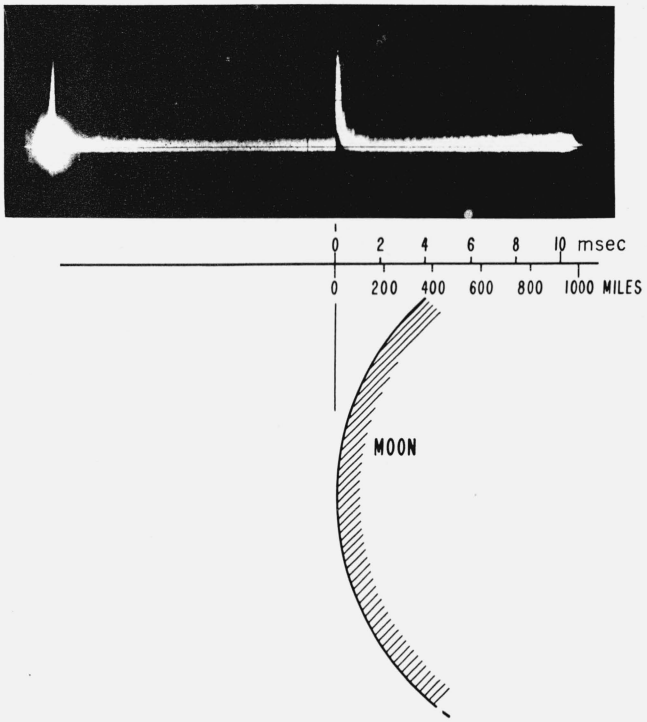

FIGURE 7. *Moon echoes observed by Trexler* [1958] *compared to scale with curvature of the moon (modified from a sketch in the IRE which had the moon radius 2000 miles).*
(Courtesy of the editors of Proc. IEEE.)

edge of the echo, but this appeared to be a function of signal-to-noise ratio. Yaplee et al., [1958], and later Hey and Hughes [1959] reported similar behavior at a wavelength of 10 cm, when 2- and 5-μsec pulses were used, respectively.

The difficulty involved in these observations is to obtain good range resolution together with adequate signal-to-noise ratio. To achieve good range resolution, one is obliged to use short pulses which (a) causes the peak echo power to fall due to a reduction in the illuminated surface area (fig. 1), and (b) requires the receiver bandwidth b to be adjusted to match the pulse length τ according to

$$b \approx \frac{1}{\tau}, \tag{15}$$

and hence makes the receiver admit more noise power as the pulse is shortened. Thus the signal-to-noise ratio falls rapidly as the pulse length is reduced and even at the present time short-pulse observations have been made only at a limited number of wavelengths, though the total cross section has been measured at many. The observations of Trexler, Yaplee, et al., and Hey and Hughes indicated that echoes come only from a portion of the surface near the center of the disk. This proved to be a consequence of the limited sensitivity of their equipment. Pettengill [1960] and Leadabrand et al., [1960] showed that echoes could be measured all the way out to the limbs with a sufficiently powerful radar system.

The first truly quantitative measurements of echo power versus delay from the leading edge to the limb were performed by Pettengill [1960] and Pettengill and Henry [1962a] at a wavelength of 68 cm using 65-μsec pulses. They employed a digital computer to average the echo intensity at range intervals of 250 μsec. Meanwhile, Hughes [1961] made observations at a wavelength of 10 cm using 5-μsec pulses and averaging the echo power by means of a single channel analog integrator with a resolution of 20 μsec. Hughes was unable to obtain echoes beyond 1 msec delay measured from the leading edge, but in the region 0–1 msec obtained results in good agreement with Pettengill and Henry [1962a]. Accordingly, he concluded that the radio-wave scattering properties of the Moon were independent of the radio wavelength λ. However, in reaching this conclusion, he ignored the fact that the resolution in the two sets of measurements was considerably different.

A search for a wavelength dependence in the scattering was undertaken by Evans [1962b, c]. A 48-channel integrator was constructed and first employed with a 30-μsec pulse radar operating at 3.6 cm. For reception, the resolution in delay was 20 μsec. Later the measurements were repeated at 68-cm wavelength with the same pulse length and resolution in delay. The two sets of measurements are compared in figure 8. A clear change in $\bar{P}(t)$ is evident. At the shorter

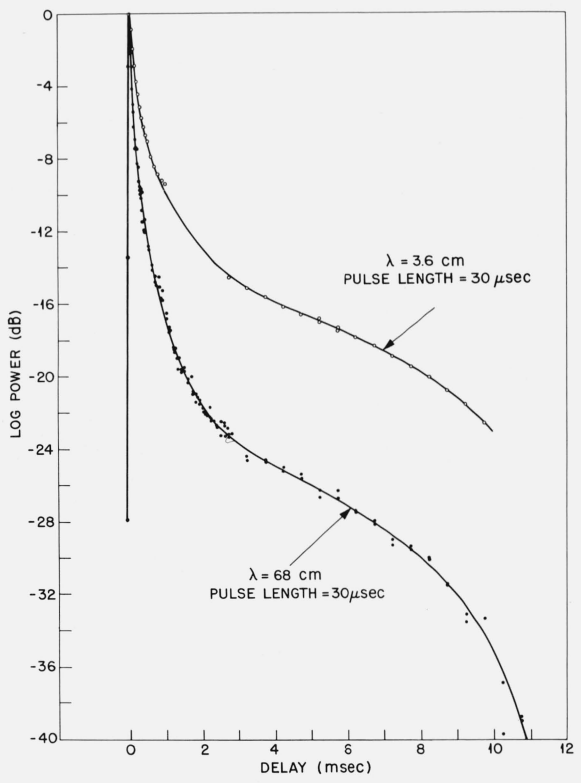

FIGURE 8. *The average echo power reflected by the moon* $\bar{P}(t)$ *as a function of delay measured with respect to the point closest to the radar.*
The 68-cm results were obtained using the same methods of averaging as were employed to obtain the 3.6-cm results. The curves have been normalized at zero delay.

wavelength, the leading edge echo is not so prominent as at 68 cm. More recent observations at a wavelength of 23 cm with the same range resolution [Evans and Hagfors, 1965] confirm the behavior shown in figure 8.

The measurements at 68 cm were later repeated with 12-μsec pulses and 10-μsec resolution in delay to achieve an overall resolution comparable to that of Hughes [1961]. A comparison of these 68- and 10-cm results is given in figure 9. Once more a clear dependence on wavelength is evident.

At longer wavelengths ($\lambda = 7.84$ m) Evans and Ingalls [1962] found that the echo power spectrum was indistinguishable from that observed at $\lambda = 68$ cm. However, Faraday fading of the echoes [Browne et al., 1956] and possibly ionospheric scintillation may have introduced error. Davis and Rohlfs [1964] have employed a 250-μsec pulse radar at 11.3-m wavelength to obtain the scattering behavior over the first 4 msec of delay. Despite the long pulse used, they found (fig. 10) that the wavelength dependence shown in figure 8 is continued in the meter-wave region. Because ionospheric scintillation effects cannot introduce systematic errors in short-pulse determinations of the scattering behavior, this seems to be the only reliable technique at these long wavelengths.

At shorter wavelengths, Lynn, Sohigian, and Crocker [1963] have determined the scattering behavior at 8.6 mm. These observations were remarkable in that a transmitter power of only 12 W was employed and that resolution of different range delays was achieved solely by means of the angular resolution afforded by the antenna beam (4.3 min arc). Thus

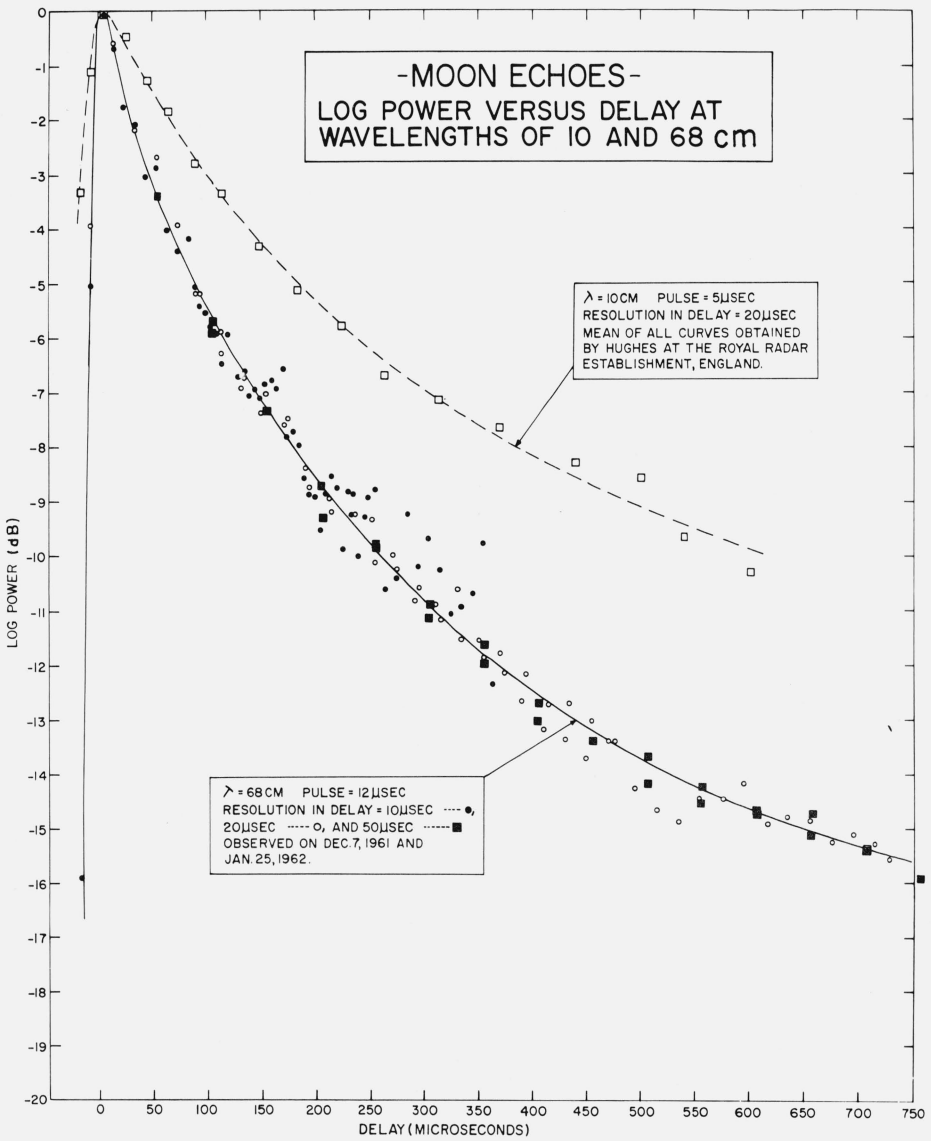

FIGURE 9. *High-resolution measurements of* $\overline{P}(t)$ *at 68-cm wavelength and at 10-cm wavelength* [*Hughes, 1961*].

As in figure 8, a clear wavelength dependence can be observed. The curves have been normalized at zero delay.

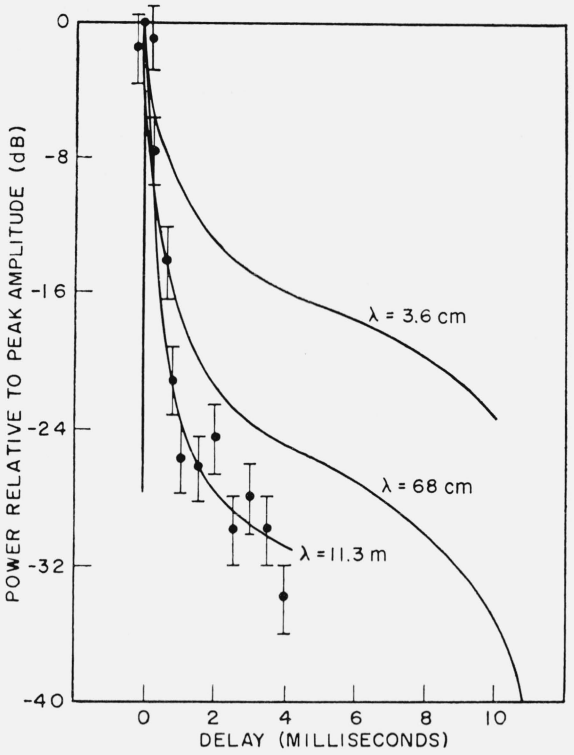

FIGURE 10. *The results obtained by Davis and Rohlfs* [1964] *at 11.3-m wavelength using 250-μsec pulses are shown here with the results presented in figure 8 for comparison.*

the antenna was directed at different distances from the center of the lunar disk to determine the brightness distribution. This achieves poor range resolution at the limbs as *equal projected* areas are illuminated as distinct from the *equal surface* area illuminated by short-pulse radars. To correct the observations at the limb for the amount of the antenna pattern projected onto the sky which provided no illumination of the Moon, Lynn, Sohigian, and Crocker [1963] assumed that the Moon behaved as a uniformly bright reflector (Lommel-Seeliger law). Their results when put in the same form as those of Evans and Pettengill [1963c] are shown in figure 11. The wavelength dependence of the scattering of electromagnetic waves by the Moon in the wavelength range 1 meter to that of light is very evident. At 8 mm only a small highlight appears at the center. The brightness there exceeds that of other regions by only a factor of two. At 3.6 cm this ratio is of the order of 25 and at 68 cm, 150. Lynn, Sohigian, and Crocker [1963] also reported that there were no differences between the brightness of the maria and the highlands larger than ($\pm$2dB)—the accuracy of their observations. It would seem that the rough structure responsible for diffuse scattering at 8.6 mm is to be found overlying highlands and maria equally. It is tempting to conclude that the microrelief responsible for the Moon's photometric properties also controls the scattering at 8.6 mm, perhaps by extending in depth to several millimeters.

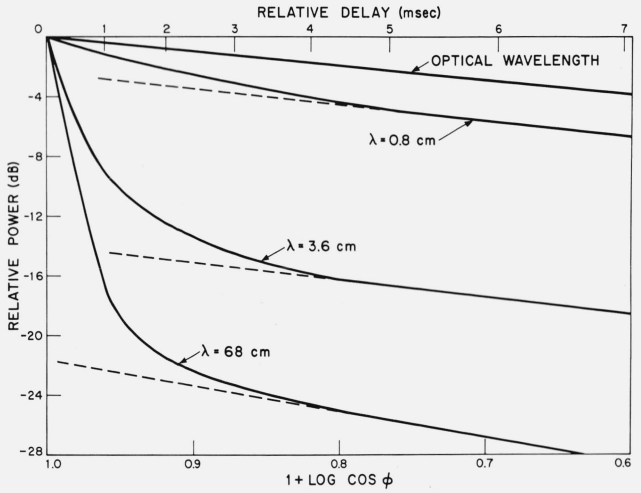

FIGURE 11. *The distribution of echo power as a function of 1 + cos φ at 8.6-mm wavelength* [*Lynn et al., 1963*].
The 3.6-cm and 68-cm results have been included for comparison.

We may summarize these results as follows. At a radio wavelength of 1 m, the Moon scatters predominantly from those regions at the center of the visible disk which are nearly normal to the line of sight. This suggests a rather smooth surface. However, as the wavelength is reduced, more and more power is returned from other regions showing that as the scale of the exploring wave is reduced, the surface is found to appear increasingly rough. At 1-cm wavelength the disk appears to be almost uniformly bright, indicating that the surface is now essentially covered with structure having dimensions comparable with the wavelength.

3.3. Orthogonal Polarization Observations

Browne et al., [1956] observed that the nulls introduced by the Faraday fading were quite deep and that the amount of depolarized power was about 10 percent. This was later confirmed by Blevis and Chapman [1960]. Senior and Siegel [1960] were the first to argue that this result alone demonstrates that the reflection occurs from largely smooth surfaces. In order to study the depolarizing ability of the lunar surface, it is desirable to overcome the Faraday fading, and this is most easily accomplished by using circularly polarized waves and receiving the circular component having the same sense as that transmitted. This experiment has been performed at 68-cm wavelength by Pettengill and Henry [1962a] using 400-μsec pulses, and later by Evans [1962c] using 200-μsec pulses. As may be seen in figure 12, the depolarized component of the power obeys the law $\bar{P}(\phi) \propto \cos \phi$, indicating that these signals are scattered equally from all parts of the projected disk. The percentage polarization can be expressed in the form

$$\text{Polarization} = \frac{\bar{P}(t) - \bar{D}(t)}{\bar{P}(t) + \bar{D}(t)} \times 100\%, \tag{16}$$

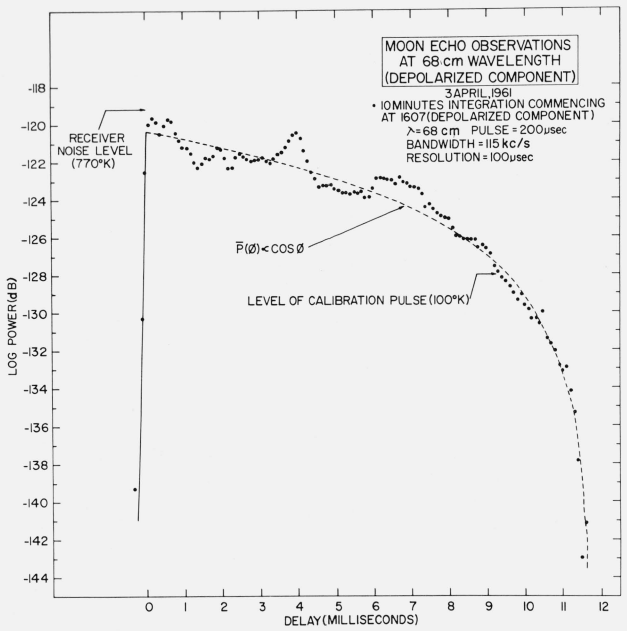

FIGURE 12. *The average echo intensity versus range delay* $\bar{D}(t)$ *for the depolarized component of the signals* [*Evans and Pettengill 1963c*].

The dotted curve indicates the expected behavior for a uniformly bright moon. The departures from the smooth curve are thought to represent the existence of departures from statistical uniformity of the surface features over the moon's disk. These might be expected to be more easily seen in the depolarized than polarized component.

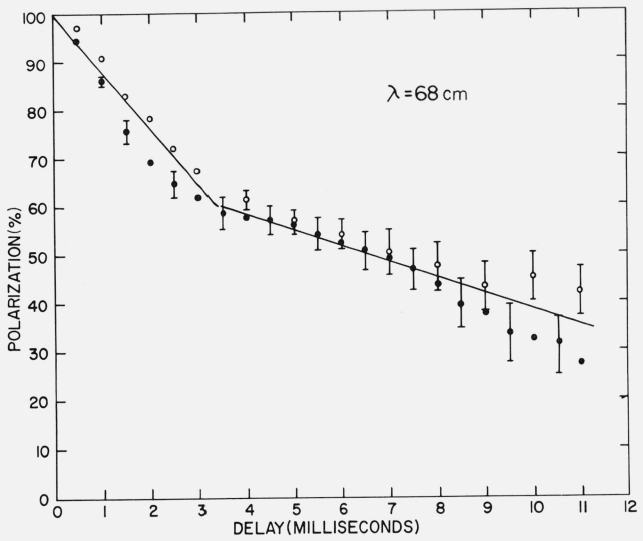

FIGURE 13. *The percentage polarization of moon echoes as a function of range delay observed at 68-cm wavelength* [*Evans and Pettengill, 1963c*].

These values were computed from the results shown in figure 12 by means of the expression (16). The earlier values obtained by Pettengill and Henry [1962a] are also shown.

where $\bar{P}(t)$ is the average polarized or expected return and $\bar{D}(t)$ the depolarized component. The percentage polarization has been plotted in figure 13 for both the 400- and 200-μsec pulse observations. It appears that the percentage polarization falls linearly out to a delay of 3 msec where it has a value of 60 percent. Beyond this value of delay the depolarization falls less rapidly, and the ratio of the amount of power in the two components $\bar{P}(t)/\bar{D}(t)$ is approximately constant at 3:1.

Two mechanisms which could give rise to depolarization are (a) multiple reflections at the surface in which one or more reflections occur near the Brewster angle, and (b) the excitation of surface elements which are comparable in size to the wavelength and reradiate as dipoles. Probably both mechanisms contribute to some extent, but (a) seems incapable of converting one quarter of the incident power into the depolarized component.

It seems that further polarization studies might be most profitable. They are capable of showing the presence or absence of a dust layer on the surface through which the radar signals may be propagated. The experiments which would need to be carried out have been considered by Hagfors (private communication).[3]

4. The Angular Scattering Laws

Evans and Pettengill [1963c] have explored a number of empirical laws by which to represent the angular power spectra $\bar{P}(\phi)$ of the signals. In this section we briefly review this work. The most obvious way to proceed is to plot the logarithm of the power against log cos ϕ to see if simple laws of the form

$$\bar{P}(\phi) \propto \cos^m \phi \qquad m = \text{constant} \tag{17}$$

can be made to fit the results. The experimental uncertainties in the measurements made to date are least in those for 68-cm wavelength. As we have seen, the depolarized component $\bar{D}(t)$ observed at this wavelength (fig. 12) is fairly well represented by this type of law where $m = 1$, i.e., indicating that the surface is uniformly bright (sec. 3.1). The polarized or expected component $\bar{P}(t)$ observed at 68 cm is shown in figure 14. It can be seen that over the region $80° < \phi < 90°$ the same law is found to hold, namely,

$$\bar{P}(\phi) \propto \cos \phi, \tag{13}$$

but for $45° < \phi < 80°$ it is found that

$$P(\phi) \propto \cos^{3/2} \phi. \tag{18}$$

This law lies midway between Lommel-Seeliger, (13), and Lambert, (14). The behavior shown in figure 14 has also been found for echoes obtained at a wavelength of 23 cm [Evans and Hagfors, 1965]. At wavelengths longer than 68 cm, the behavior of this tail region of the echo has not yet been reported.

At shorter wavelengths, e.g., $\lambda = 3.6$ cm, the measurements are somewhat less reliable due to the difficulties involved [Evans and Pettengill, 1963c] but indicate that for $60° < \phi < 90°$ the Lommel-Seeliger law, (13), holds. That is, the limb region appears uniformly bright (fig. 15). The same behavior is inferred at a wavelength of 8.6 mm (see fig. 11), though the poor resolution of the limb region obtained in these measurements makes it difficult to be certain that this is so.

[3] See note added in proof.

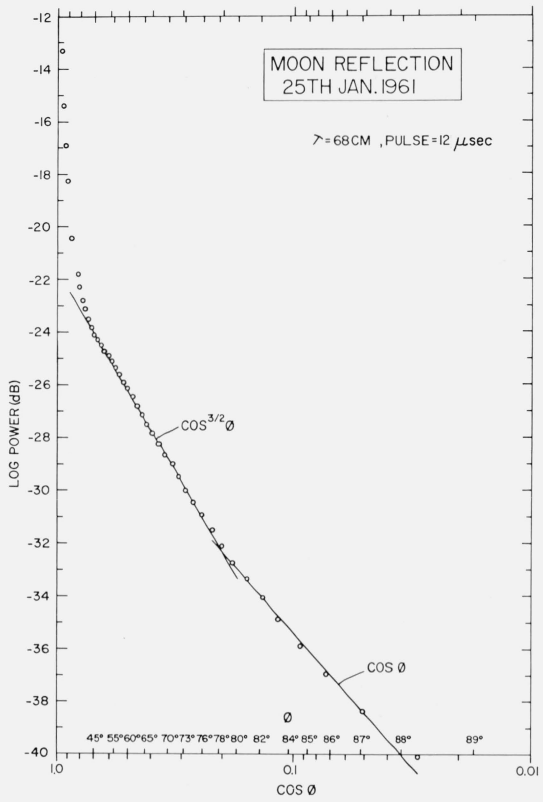

FIGURE 14. *The average echo power* $\bar{P}(\phi)$ *plotted as a function of log cos* ϕ *for observations at 68-cm wavelength with 12-*μ*sec pulses.*

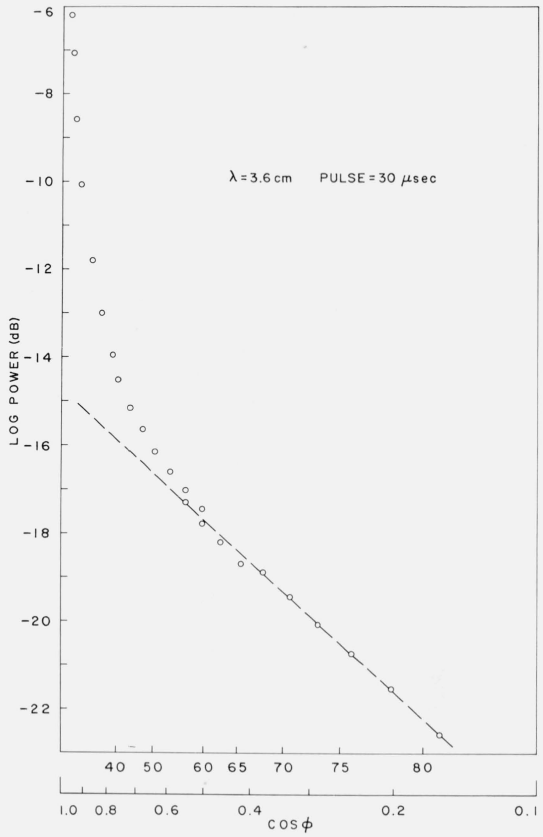

FIGURE 15. *The average power* $\bar{P}(\phi)$ *plotted as a function of log cos* ϕ *for observations at 3.6-cm wavelength with 30-*μ*sec pulses.*

The Lambert law might be expected to hold where the surface is covered with irregularities of comparable size to the wavelength. The Lommel-Seeliger law could be expected to hold where the elements of the surface are largely smooth but arranged with a wide range of slopes. Thus near the limbs one sees elements normal to the line of sight and these screen from view regions which would not reflect favorably. The $\cos^{3/2}\phi$ dependence observed at 68 cm and 23 cm has not been satisfactorily explained at the present time. Evans and Pettengill [1963c] supposed that it might represent a combination of Lommel-Seeliger and Lambert scattering. They termed this component of the echo power "diffuse" to distinguish it from that observed for $\phi < 45°$ where the angular dependence is steep.

When the diffuse components of the echo power obeying the $\cos^{3/2}\phi$ or $\cos\phi$ laws have been subtracted from the total, the remainder represents the power attributable to the central portions of the lunar surface. The marked dependence of this component upon the angle of incidence and reflection ϕ caused Evans [1957, 1962a; Pettengill, 1960; Pettengill and Henry, 1962a] to describe it as a "specular" component. This term has given rise to some confusion, and as it was not intended to convey that the Moon is perfectly smooth, we shall here use the term "quasi-specular."

The observations of the orthogonal component $\bar{D}(t)$ unfortunately have only been conducted at a wavelength of 68 cm at the present time. They do, however, strengthen the case for treating the polarized return as the superposition of two components, as approximately one-third of the "diffuse" echo power is observed when the depolarized component is examined. This seems to support the view that the "diffuse" component is due to scattering from components of the surface structure which are small-scale elements of a whole distribution of structure sizes [Evans and Pettengill, 1963c; Fung and Moore, 1964]. It seems probable that this structure can be identified with the numerous small craters that are found on the surface of the Moon and whose number increases rapidly with diminishing size.[4]

The quasi-specular component at 68-cm wavelength was observed by Pettengill and Henry [1962a] to obey a law of the form

$$\bar{P}(\phi) \propto \exp(-10.5 \sin\phi), \tag{19}$$

and a similar dependence was obtained by Hughes [1961]. However, Evans and Pettengill [1963c] showed that the law observed for the quasi-specular

[4] See note added in proof.

component at 68 cm changes with pulse length as

65-μsec pulses $\quad \bar{P}(\phi) \propto \exp(-10.5 \sin \phi)$
$7.5° < \phi < 60°$ (19)

30-μsec pulses $\quad \bar{P}(\phi) \propto \exp(-12.5 \sin \phi)$
$5° < \phi < 12°$ (20)

12-μsec pulses $\quad \bar{P}(\phi) \propto \exp(-15.3 \sin \phi)$
$3° < \phi < 9°$. (21)

As the pulse is shortened, the exponent increases and the range of angles over which the law holds decreases. Thus, Evans and Pettengill [1963c] concluded that a law of this form had no general validity, and instead proposed a law of the form

$$\bar{P}(\phi) \propto \frac{1}{1+b\phi^2}, \tag{22}$$

where b is a constant. However, a recomputation of the power in the quasi-specular component (shown in fig. 16) indicates that this law also is a poor fit. A good fit to the experimental results can be obtained from a theoretical treatment of the scattering from a rough surface as described in the next section. As yet, no very simple empirical law has been found which by adjusting only one parameter can be made to fit the quasi-specular component at all wavelengths.

5. The Scattering Behavior of an Irregular Surface

We have seen from the results presented in the two previous sections that the way in which the Moon scatters radio waves is distinctly different from the manner in which it reflects light. For wavelengths of 1 m or longer, the Moon appears to be a very limb dark reflector whereas optically it is almost uniformly bright [Markov, 1948]. One may conclude, therefore, that on a scale of 1 m the Moon is much smoother than on a scale of a few microns. The extent to which it is possible to deduce the statistical properties of the lunar surface from these results can only be reviewed briefly here.

The simplest type of theory is one involving geometric optics and has been adopted by a number of authors [Brown, 1960; Muhleman, 1964; Rea, Hetherington, and Mifflin, 1964]. This has the virtue of avoiding a difficulty encountered in the other treatments, namely, that the reflection coefficient will be a function of the angle of incidence and reflection. This difficulty has caused several authors to treat the Moon as an irregular *perfectly conducting* sphere—which is clearly not the case. In the geometric-optics approach only surfaces normal to the line of sight scatter back favorably, and their reflection coefficient is simply the Fresnel reflection coefficient for normal incidence ρ_0. This approach can be outlined as follows. We pass a vertical plane through the surface and examine the distribution of the slopes in this plane. If the probability of finding an elemental length dS (measured

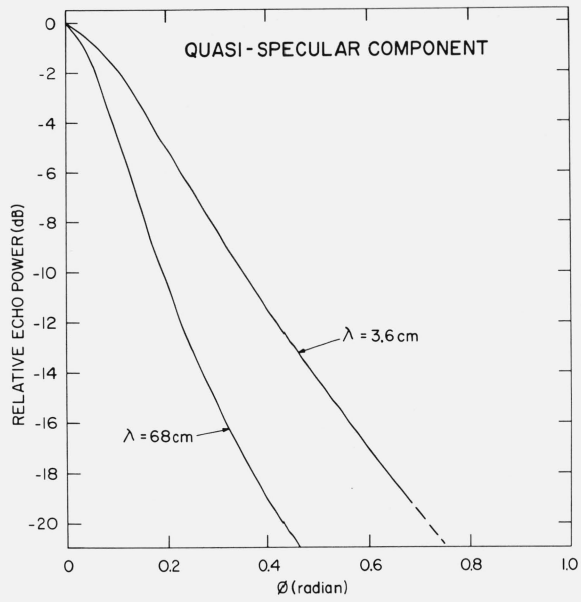

FIGURE 16. *The quasi-specular component of lunar echoes at 3.6- and 68-cm wavelength.*
These curves were obtained from the results shown if figures 14 and 15 after subtracting the component of power which conforms to the straight lines in those plots. The quasi-specular component is believed to be attributable to the reflections from the large-scale, smooth, undulating parts of the surface.

along the mean surface and not the actual surface) associated with a slope in the range ϕ to $\phi + d\phi$ between the actual surface and the mean is $f(\phi)d\phi$, then the angular power spectrum $\bar{P}(\phi)d\phi$ is given in

$$P(\phi)d\phi \propto \frac{f(\phi)d\phi dS}{\cos \phi}. \tag{23}$$

It follows that the distribution of surface slopes $f(\phi)\,d\phi$ and the mean slope $\bar{\phi}$ can be obtained directly from the radar measurements of the angular power spectrum $\bar{P}(\phi)$ (sec. 6). One would expect a law of the form (23) to describe only the scattering from the large smooth elements of the surface which give rise to the quasi-specular component of the echo (fig. 16). This follows because a geometric-optics treatment is applicable only to the extent that the surface can be regarded as gently undulating, and makes no allowance for small-scale structure (which would cause diffraction) and shadowing effects. It is clear from the wavelength dependence of the scattering (sec. 3) that the Moon's surface does have a considerable amount of structure with dimensions comparable to the wavelength, and it follows that this must become increasingly important as $\phi \rightarrow 90°$.

Other workers have chosen to treat the surface as being *perfectly conducting*, *smooth* and undulating, and causing no shadowing. The requirement that the surface be smooth is here intended to mean that it contain no structural components having horizontal and vertical dimensions comparable with the wavelength, since the boundary conditions are established locally by means of Fresnel's reflection formulae. It is next commonly assumed [e.g., Hargreaves, 1959; Daniels, 1961; Hagfors, 1961; Winter,

1962] that the departure of the true surface from the mean follows a Gaussian probability distribution. That is, the chance of finding a given point to be at a height h above the mean surface is proportional to $\exp[-\frac{1}{2}(h/h_0)^2]$ where h_0 is the rms height variation. Other forms of height distribution [Bramley, 1962] have been used, but the theory should not be very sensitive to this function provided $h_0 >> \lambda$ [Hargreaves, 1959; Daniels, 1961, 1962]. This follows because the phase variation in the reflected wave front will be many times 2π rad when $h_0 >> \lambda$ and it becomes impossible to determine h_0 from the observations. Having described the vertical behavior of the surface, it remains only to describe its horizontal structure. This is done by means of an autocorrelation function $\rho(d)$ where

$$\rho(d) = \frac{\overline{h(x)h(x+d)}}{(h_0^2)}, \tag{24}$$

in which $h(x)$ is the height of the surface at a point x and $h\ (x+d)$ at a distance d away. The case where $\rho(d)$ is another Gaussian function,

$$\rho(d) \propto \exp\left[-\frac{1}{2}\left(\frac{d}{d_0}\right)^2\right], \tag{25}$$

in which d_0 is the horizontal scale size, has been treated by Hargreaves [1959] and Hagfors [1961]. If the surface be considered plane and extending in one direction only, then each point on the surface introduces a phase change in the reflected wave of $(4\pi h/\lambda)\cos\phi$ radians. These phase fluctuations are said to be shallow if the rms phase fluctuation $\Omega = (4\pi h_0/\lambda)\cos\phi$ is less than 1 rad, and in this case the autocorrelation function describing the variation of radio phase with distance d over the surface will be the same as $\rho(d)$. If, on the other hand, $h_0 >> \lambda$, the rms phase fluctuation Ω becomes greater than 1 rad and the correlation distance in the reflected phase front will fall from d_0 to d_0/Ω (since 0, 2π, 4π, . . . radians are indistinguishable). At a large distance from the surface, the initial phase variations become modified due to the overlapping of many rays, and amplitude fluctuations appear. An rms phase fluctuation $\Omega/\sqrt{2}$ is then observed [Bowhill, 1957].

The angular power spectrum $\sigma(\phi)$ is given by the Fourier transform of the autocorrelation function describing the reflected phase front immediately after reflection, and can be written

$$\sigma(\phi) \propto \exp[-\tfrac{1}{2}(\phi/\phi_0)^2], \tag{26}$$

where $\phi_0 = \lambda/2\pi d_0$ for $h_0 << \lambda$ and $\phi_0 = h_0/d_0$ when $\lambda << h_0$. It follows that where the wavelength is much larger than the vertical extent of the height fluctuations, the value of ϕ_0 yields directly the horizontal scale of the structure. When $\Omega \geq 1$ rad, ϕ_0 yields only the ratio h_0/d_0. Since h_0/d_0 is the mean surface gradient, this means that only the rms surface slope can be determined, but not the actual horizontal or vertical scale sizes. If observations could be made as the wavelength was increased, eventually (when $\lambda > h_0$) it would be possible to determine d_0. However, in the case of the Moon this would require low-frequency radio waves which could not propagate through the earth's ionosphere. Daniels [1961, 1962] has discussed at length this limitation in radar observations and shown that one cannot obtain information on the rms height fluctuation when this is many times the wavelength in size. It is also clear that small-scale height fluctuations $\leq \lambda/8$ will introduce only small phase changes in the reflected phase front and will be unimportant. Thus radar observations may be regarded as being sensitive to structure in the range $\lambda/8$ to about 100 or so wavelengths. Only by repeating the observations over a wide range of wavelengths can the true nature of the surface be determined.

Other forms than Gaussian for the autocorrelation function $\rho(d)$ have been explored. These include exponential,

$$\rho(d) \propto \exp(-d/d') \tag{27}$$

[Daniels, 1961; Hayre and Moore, 1961; Hughes, 1962a, b], which closely approximates many terrestrial surfaces. Fung and Moore [1964] and Beckmann [1964a, b] have employed a sum of such terms.

When allowance is made for the curvature of the Moon's surface, and the physically most plausible series of approximations for the terms in the expression for the reflected field (Huygen's integral) are made, the following results are obtained [Hagfors, 1964]:

Gaussian $\quad \rho(d) \propto \exp\left[-\frac{1}{2}\left(\frac{d}{d_0}\right)^2\right]$ (25)

$$\sigma(\phi) \propto \frac{\exp[-\phi^2/2\phi_0^2]}{\cos^4\phi} \tag{28}$$

where $\phi_0 = h_0/d_0$

Exponential $\quad \rho(d) \propto \exp(-d/d')$ (27)

$$\sigma(\phi) \propto \left\{\frac{1}{\cos^4\phi + C\sin^2\phi}\right\}^{3/2} \tag{29}$$

where $C = [d'\lambda/4\pi h_0^2]^2$.

Hagfors [1965] has shown that if the statistics of the surface slopes are made the same, then the geometric-optics approach outlined earlier can be made to yield precisely these same results. Hence, the two approaches are equivalent.

If one reexpresses (29) for the case where ϕ is small, a simpler expression can be obtained,

$$\sigma(\phi) \propto \left\{\frac{1}{1+(C-2)\phi^2 - \frac{(C-5)}{3}\phi^4}\right\}^{3/2}. \tag{30}$$

The experimental results for the quasi-specular component observed at 68- and 3.6-cm wavelength

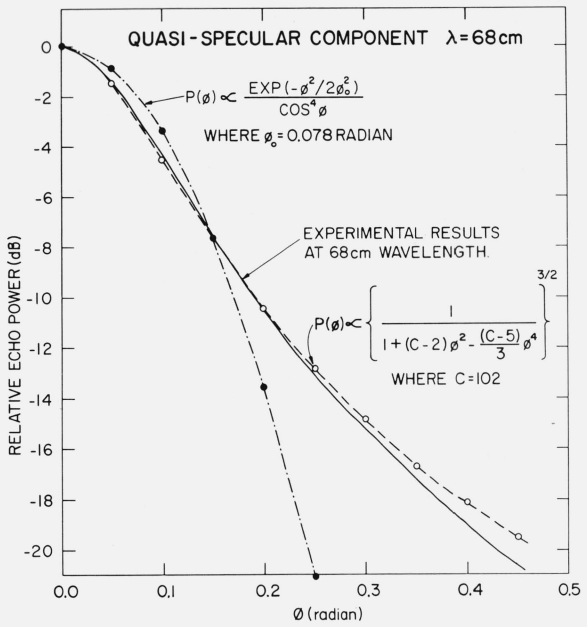

FIGURE 17. *The values obtained for the echo intensity at 68 cm using 12-μsec pulses (after the cos φ and cos$^{3/2}$ φ components shown in figure 14 have been removed) compared with the theoretical laws for the angular dependence of the reflected power.*

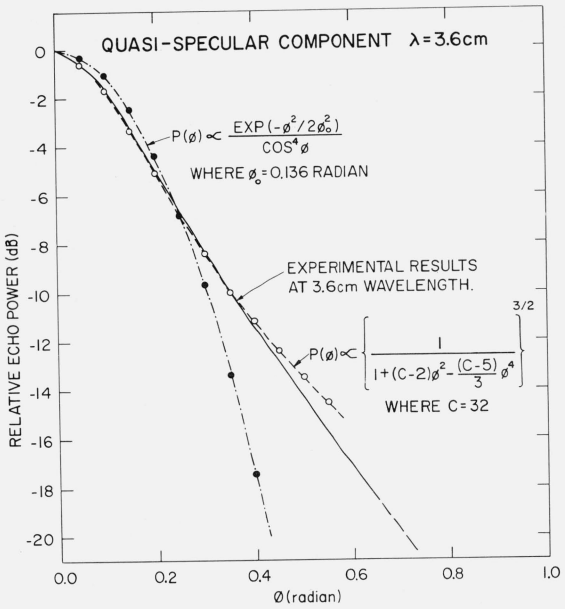

FIGURE 18. *The values obtained for the echo intensity at 3.6 cm (after the cos φ component shown in figure 15 has been removed) compared with the best-fitting curves for the theoretical laws predicted for a surface having a lateral correlation of surface heights that is a Gaussian or exponential.*

are compared with the closest-fitting curves corresponding to the laws expressed in (28) and (30) in figures 17 and 18. At both wavelengths the exponential result, (30), provides a much better fit to the measurements than the Gaussian model for the surface autocorrelation function.

In the exponential model the constant C in (30) contains the wavelength λ. Thus we would expect C to vary as λ^2, yet this does not appear to occur. We must conclude that, though the model employing the exponential autocorrelation function to describe surface roughness appears to provide a better fit at both wavelengths, it is not characterized by the same value of d'. Presumably the change in wavelength makes the reflection properties of the surface dependent on a different range of structure sizes. Some authors [Muhleman, 1964; Fung and Moore, 1964; and Beckmann, 1964a, b] have not distinguished between the diffuse and quasi-specular scattering, and have attempted to fit their theoretical results to the whole curve for $\bar{P}(\phi)$. In some cases they have been surprisingly successful and have argued that this demonstrates that the distinction between the two regimes is artificial. Unfortunately, each author has commenced by assuming that the surface is locally smooth and no theory has properly attempted to account for small-scale structure, diffraction, and shadowing effects. These must be important as $\phi \rightarrow 90°$ and it seems a doubtful procedure to conclude that the theory is adequate, simply because it can be made to match the results by empirically adjusting two or more constants.

At the present time, experimental approaches are being employed in some laboratories to gain a better knowledge of the relation between the statistical properties of a surface and its scattering behavior. In this work a surface is modeled (usually in sand) over a large area of floor space and the scattering properties explored at millimeter wavelengths.

On a somewhat larger scale, observations of the scattering behavior of the Earth's surface conducted using airborne radar equipment can assist in interpreting the lunar echoes. We note that these airborne studies indicate that marked "quasi-specular" behavior is encountered only over deserts or moderately calm sea [Grant and Yaplee, 1957; Edison, Moore, and Warner, 1959].

6. Surface Slopes

From the 68-cm results presented in section 3, different workers have derived values for the average surface slope in the range 5° and 15°. In part this wide scatter of values reflects differing interpretations of the results. For example, Muhleman [1964] has averaged over the whole $\bar{P}(\phi)$ curve whereas Evans and Pettengill [1963c], Rea, Hetherington, and Mifflin [1964], and Daniels [1963b] have attempted to subtract out the diffuse component of the echo power before computing the slope. Differences also have arisen because most authors weight the values for the slope by the amount of area projected on to the mean surface associated with that slope; yet others, e.g., Rea, Hetherington, and Mifflin [1964] weight by the actual amount of area at each slope. The first method is in

TABLE 3. *Values for the rms or average slope of the undulating part of the lunar surface derived by different authors from radar reflection measurements in the wavelength range 3 m to 10 cm*

Author	Meter wave values for the average slope	Wavelength	Comments
Hargreaves [1959]	6°	2.5 m	RMS value obtained by "Gaussian" fit to data published by Evans [1957].
Hagfors [1961]	4°	3 m	RMS value obtained by "Gaussian" fit to the data published by Evans et al., [1959].
	3°	68 cm	RMS value obtained by "Gaussian" fit to the data published by Hey and Hughes [1959].
Daniels [1961]	8–12°	68 cm	Average value obtained by "exponential" fit to data published by Pettengill [1960].
Daniels [1963a]	14°	70 cm	Average value obtained by "exponential" fit to data of J. V. Evans (private communication).
Daniels [1963b]	6.5°	70 cm	Average value after correcting results of Daniels [1963a] for the diffuse component.
Hey and Hughes [1959]	3°	10 cm	RMS value obtained by "Gaussian" fit to own data.
Evans and Pettengill [1963c]	4.5°	68 cm	RMS value obtained by "Gaussian" fit to own data.
	5°	68 cm	Average value obtained by "exponential" fit to own data.
Muhleman [1964]	8°	68 cm	RMS value obtained by "Gaussian" fit to results of Pettengill [1960]. Includes diffuse component.
	7°	68 cm	Average value obtained by "exponential" fit to results of Pettengill [1960].
Rea et al., [1964]	11°	68 cm	Average value obtained for results of Evans and Pettengill [1963c] when diffuse power subtracted.*
	15°	68 cm	RMS value obtained for results of Evans and Pettengill [1963c] when diffuse power subtracted.*

*Here the slope has been defined somewhat differently—see the text.

effect a value for the slope that would be deduced by repeatedly dropping down onto the Moon, and the second after walking over the surface and measuring the slopes.

Table 3 lists some of the values for the rms or average slope of the lunar surface that have appeared in the literature. They refer to measurements made in the wavelength range 3 m to 10 cm and hence are roughly comparable. It seems that with the possible exception of the results published by Rea, Hetherington, and Mifflin [1964], none of the values in table 3 are close to the value that would be encountered by a landing vehicle. This follows because most authors have computed the average of the slopes encountered when passing a vertical plane through the surface. Thus, in the geometric-optics approach, the mean slope $\bar{\phi}$ has been taken as

$$\bar{\phi}=\frac{\int_\phi \phi f(\phi)d\phi}{\int_\phi f(\phi)d\phi}=\frac{\int_\phi \phi\bar{P}(\phi)\cos\phi d\phi}{\int_\phi \bar{P}(\phi)\cos\phi d\phi}, \tag{31}$$

which follows directly from (23). However, the slope encountered in any plane cut through the surface is not necessarily the steepest gradient for that facet, and to obtain the true mean slope encountered by a landing vehicle, one must pass the vertical plane through the surface at all possible azimuth angles. That is, the most meaningful value for $\bar{\phi}$ is given in

$$\bar{\phi}=\frac{\int_\phi \phi f(\phi)\sin\phi\, d\phi}{\int_\phi f(\phi)\sin\phi\, d\phi}=\frac{\int_\phi \phi\bar{P}(\phi)\cos\phi\sin\phi\, d\phi}{\int_\phi \bar{P}(\phi)\cos\phi\sin\phi\, d\phi}. \tag{32}$$

As stated earlier, it is our view that the function $\bar{P}(\phi)$ employed in (23) should not be the whole curve but one corrected for the presence of the diffuse component (e.g., the curves shown in fig. 16).

Essentially the same difficulty in defining what is meant by the mean slope has arisen when an autocorrelation function has been used to describe the surface. Thus in the Gaussian case the ratio h_0/d_0 is the rms slope only when the distribution is examined in a single vertical plane, and when all such planes are averaged, the rms slope is found to be $\sqrt{2}h_0/d_0$ [Hagfors, 1965]. In the case of the exponential autocorrelation function, the relation between the constant C which appears in (30) and the mean slope has been shown by Hagfors [1965] to be

$$\overline{\tan\phi}\approx\frac{1}{2\sqrt{C}}\cdot\frac{C-4}{C-\sqrt{C}-2}\cdot\log_e 4C. \tag{33}$$

Equation (33) holds only for large values of C (>100) and Hagfors [1965] concurs with the view of Rea, Hetherington, and Mifflin [1964] that to characterize the slopes by a single number is almost certainly misleading. The most meaningful statement is a curve of $\bar{P}(\phi)\cos\phi$ which may be taken as the probability distribution encountered in a single plane. The results for $\bar{P}(\phi)$ shown in figure 16 have been employed in (32) to yield values for the mean slope $\bar{\phi}$ by numerical integration. The results are at $\lambda=68$ cm, $\bar{\phi}=10.2°$, and $\bar{\phi}=14.8°$ *at* $\lambda=3.6$ cm. These values are probably overestimates since the behavior of $\bar{P}(\phi)$ for $\phi<2.5°$ has not properly been explored due to the finite width of the pulse. The mean slope is evidently a function of wavelength, and this reflects the fact that each wavelength acts as a filter and is sensitive only to a given range of structure sizes. It seems probable that the slope obtained by the procedure outlined here will be determined principally by elements of the surface of the order of 10 λ across. Thus the average slope observed at 68 cm (10.2°) seems the appropriate value to employ, for example, for the design of a lunar landing craft.

7. The Dielectric Constant *k*

In section 2 we introduced two generalized radar equations for an irregular sphere,

$$\sigma=g\rho_0\pi a^2 \tag{8}$$

and

$$\sigma=G_m\bar{\rho}\pi a^2. \tag{10}$$

786-228 O-66-10

We have seen from the foregoing results that the Moon appears to scatter in part as a smooth undulating sphere and in part as a collection of small-scale, almost isotropic, scatterers. At 68-cm wavelength the ratio of the powers due to these two parts is 4 : 1. In attempting to derive a value for the dielectric constant k, Evans and Pettengill [1963c] supposed that a fraction X of the actual surface area could be associated with the diffuse component, and further that these scatterers obeyed the Lambert law, (14), for which the gain $G_m = 8/3$ [Grieg, Metzger, and Waer, 1948]. The remainder of the surface they took to be smooth and undulating and assumed it to have a directivity factor $g \rightarrow 1.0$. Hagfors [1964] has since shown that $g = 1 + \alpha^2$ for the smooth part of the surface where $\alpha = h_0/d_0$ for a Guassian surface (25) and hence is related to the rms slope (sec. 6). Since $\alpha \sim 0.1$ at $\lambda = 68$ cm, it follows that $g \rightarrow 1.0$, and the assumption $g = 1.0$ made by Evans and Pettengill [1963c] is not a bad one. The total cross section σ was thus obtained as the sum of two parts, the smoother being obtained from (8) and the rough from (10),

$$\sigma = \left[(1 - X)\, \rho_0 + \frac{8}{3} X \bar{\rho} \right] \pi a^2. \tag{34}$$

With no real justification, Evans and Pettengill [1963c] equated $\bar{\rho}$ to ρ_0, since otherwise (34) cannot be solved. The error introduced into the value for the dielectric constant k is likely to be small because the second term in (34) has a value of only 1/4 of the first. However, the value for X (which is found to be 8 percent) might be somewhat in error. At all events the cross section was then written

$$\sigma = \left[(1 - X) + \frac{8}{3} X \right] \rho_0 \pi a^2 = 0.074\ \pi a^2. \tag{35}$$

From this ρ_0 was found to be 0.065, and this led to a dielectric constant $k = 2.79$. Evans and Hagfors [1964] applied these arguments to the observations conducted at 3.6 cm and 8.6 mm to obtain the results shown in table 4.

TABLE 4. *Values for the reflection coefficient at normal incidence ρ_0 and dielectric constant* k *deduced by Evans and Hagfors [1964]*

Wavelength	Power in the diffuse component	X	ρ_0	k
cm	%	%		
68	20	8	0.065	2.79
3.6	30	14	.060	2.72
0.86	85	68	.035	2.13

We have remarked that, provided the amount of power in the diffuse component remains small, this series of approximations probably does not introduce serious error in the value for k, although the percentage area of the surface X that is rough may be in error. When the largest part of the power appears in the diffuse component (e.g., at 0.86 cm) it is doubtful that (35) has much validity. Hence, little significance should be attached to the apparent wavelength dependence in k shown in table 4. If the wavelength dependence could be shown to be real, it might result either as a consequence of a finite conductivity s in the medium [see (6)], or the surface may be inhomogeneous and have density variations with depth.

A somewhat more rigorous approach to the problem of dealing with the smooth and rough portions of the surface has been published by Rea, Hetherington, and Mifflin [1964]. In this approach the Moon is assumed to be covered with equal-sized flat facets having a distribution of slopes $f(\phi)$. The cross section can then be computed and the directivity g is found to be simply the ratio of the actual area to the projected area (i.e., $2\pi \int_0^{\pi/2} f(\phi) \sin \phi\, d\phi$). In order to obtain $f(\phi)$, Rea, Hetherington, and Mifflin [1964] subtracted from the observed echo power function $\bar{P}(\phi)$ the power in the orthogonal component $\bar{D}(\phi)$. In this way they sought to remove the influence of the small-scale roughness in determining $f(\phi)$. Since it is not clear what fraction of the incident energy one might expect to appear in the depolarized component, several possibilities were tried, namely:

Case 1, $f(\phi) \propto \bar{P}(\phi)$
Case 2, $f(\phi) \propto \bar{P}(\phi) - \bar{D}(\phi)$
Case 3, $f(\phi) \propto \bar{P}(\phi) - 2\bar{D}(\phi)$
Case 4, $f(\phi) \propto \bar{P}(\phi) - 3\bar{D}(\phi)$.

If we assume that at the limb only small-scale elements contribute to the scattering, then we might expect Case 4 to be closest the truth. This follows from the results of section 3 which showed that the ratio of $\bar{P}(\phi)$ to $\bar{D}(\phi)$ at the limb is approximately 3 : 1. Rea, Hetherington, and Mifflin [1964] concluded that the actual case lay between 3 and 4 by a similar process of reasoning. The fraction of the total power remaining for Case 4 was found to be 0.85, and the directivity factor g determined by graphical integration was 1.11. By assuming a total cross section $\sigma = 0.074\ \pi a^2$, the corresponding reflection coefficient ρ_0 was found to be 0.057, leading to a dielectric constant $k = 2.6$. Since the depolarized component $\bar{D}(\phi)$ has only been determined at 68 cm, this interesting approach cannot yet be applied to the measurements at other wavelengths.

The low value of the dielectric constant observed here is in fact somewhat larger than most values inferred from passive radio observations. Russian workers [Troitsky, 1962; Salomonovich and Losovsky, 1962; Soboleva, 1962; and Krotikov and Troitsky, 1962] arrive at values less than 2 and often of about 1.7 ± 0.2. The most recent value reported by American observers [Heiles and Drake, 1963] was 2.1 ± 0.2.

Recently, Hagfors et al. [1965][5] have carried out an experiment which appears to resolve the descrepancy. It appears that the lunar surface is inhomogeneous and that the radiometer value $k = 1.7$ applies to the uppermost layer.[6]

[5] Hagfors, T., R. A. Brockelman, H. H. Danforth, L. B. Hanson, and G. M. Hyde (1965), Tenuous surface layer on the moon. Evidence derived from radar observations, Science (in press).

[6] This experiment is discussed further in the note added in proof.

This value is so low in comparison with most of the values for terrestrial rocks listed in table 2 that we are forced to conclude that the material is extremely porous.

8. The Packing Factor of the Lunar Material

Some constraints can be placed on the packing factor W_0 which describes the fraction of the volume occupied by the material. If W_0 is small, then it seems that an expression developed by Twersky [1962] which relates the observed dielectric constant k_{obs} to that of the material in bulk should apply. If the surface is assumed to consist of grains of pure dielectric material whose size is small compared with the wavelength, and which are well separated so that they can act as independent dipoles, the observed dielectric constant will be

$$k_{obs}=1+\frac{3E}{1-E} \text{ where } E=\frac{W_0(k-1)}{k+2}, \qquad (36)$$

in which k is the dielectric constant of the material in bulk. Where W_0 is large and the surface can more properly be modeled as a continuous dielectric with small, well-separated cavities embedded in it (which now act as the scatterers), then a formula developed by Odelevskii and Levin [see Krotikov and Troitsky, 1962] should apply:

$$k_{obs}=k\left\{1-\frac{3(1-W_0)}{\frac{2k+1}{k-1}+(1-W_0)}\right\}. \qquad (37)$$

The two formulae can be shown to be equivalent by regarding the holes in the second model as vacuum spheres suspended in a dielectric and using (36) to recover (37). In figure 19 we have plotted k_{obs} versus W_0 as obtained from both equations for quartz ($k=4.0$). Also shown are some experimental results obtained by Brunschwig et al., [1960] for dry terrestrial sand. It appears from this comparison that (37) provides a much closer fit to the experimental results. It is evident from figure 19 that the value $k=1.7$ observed for the topmost layer corresponds to a packing factor $W_0=0.30$. Since quartz has a rather low value at k (see table 2) this may perhaps be taken as an upper limit to W_0 for the topmost surface. A lower limit may be obtained by taking $k=20$ whence W_0 is about 0.10.

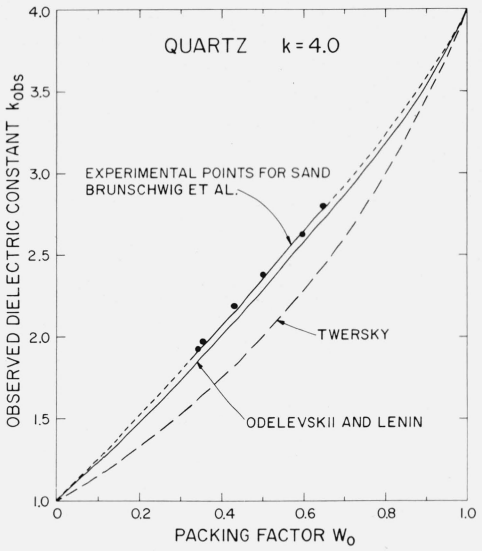

FIGURE 19. *The variation of the observed dielectric constant* k_{obs} *with the packing factor* W_0 *of a material having a bulk value of dielectric constant* $k=4$.

The packing factor W_0 is defined as the ratio of the density of the actual broken material to the material in bulk. The results obtained from two theoretical formulas (36) and (37) are here compared with experimental results reported by Brunschwig et al. [1960] for sand.

9. Coherent-Pulse Radar Observations

When a radar system is so designed that the transmitter and receiver frequencies are determined by very stable oscillators (preferably the same one), it becomes possible to derive spectral information from the phase of the signal. This is achieved by replacing the normal rectifier at the output of the receiver by two phase detectors which mix the incoming signals at a radial frequency near ω rad/sec with sin ωt and cos ωt, respectively. The outputs of these two detectors are the sine and cosine components of the signal.

For CW radar observations, the amplitude of the sine and cosine components of the signal can be determined at intervals by means of two sampling voltmeters. The sampling may be thought of as resembling the lines ruled on a spectrum grating. The longer the train of samples (number of lines), the greater will be the resolution obtained. Thus, if samples are taken over a period of 10 sec, a spectral resolution of 1/10 c/s can be achieved. The spacing of the samples ($1/f_s$) determines the spacing of the "orders" in the spectrum. Thus, if no orders are to overlap, it is required that $f_s \geq f_{max}$ where f_{max} is the frequency difference between the lowest and highest frequency components in the signal. The power spectrum $\bar{P}(f)$ in figure 5 shows the Doppler broadening of radar signals at 440 Mc/s determined by this technique.

For pulse observations it becomes possible to obtain simultaneously range and frequency resolution by phase coherent observations. This technique was first exploited by Pettengill [1960] and Pettengill and Henry [1962b]. When pulse observations are made, the sample frequency f_s automatically becomes the same as the pulse-repetition frequency. Thus the pulse-repetition frequency must be made higher than the spectral width of the signals. As the radar-wave frequency is increased, this eventually will lead to a situation where the interpulse period T becomes shorter than the radar depth of the target. In the case of the Moon, the interpulse period T must be greater than 11.6 msec. The Doppler width of the spectrum for a wave frequency of 100 Mc/s is rarely larger than 2 c/s so that difficulties are not usually encountered

786-228 O-66-11

at frequencies of less than 5,000 Mc/s, provided that the gross Doppler shift is properly compensated.

Figure 4 shows that when Doppler and range resolution are combined, it is possible to isolate localized regions of the lunar surface. If the antenna beamwidth is large with respect to the Moon, there will always be two such regions for given range and Doppler coordinates (except along the apparent equator). In the earliest work reported by Pettengill [1960] a Doppler resolution of 1/10th of a cycle was achieved from observations lasting 10 sec, and as such, each cell in the range-Doppler grid was effectively sampled only once. That is, the rms scatter in intensity was equal to the mean. By repeating the observations and superimposing 20 images, Pettengill and Henry [1962b] were able to reduce the rms fluctuation (to a factor of 2/9 the mean power). These workers also made measurements on the orthogonal component of the signal $D(\tau)$, (fig. 12) where the dynamic range encountered is much less. During the course of one afternoon's observations, Pettengill and Henry [1962b] observed a strong echo in both the expected and orthogonal component of the signals at a delay of about 2.85 msec (fig. 20) which had an intensity of about 7 to 8 times the mean at that range. They were able to resolve the ambiguity in the position of this scatterer by observing its change in Doppler frequency with respect to the center with time (as a consequence of the projection of the Moon's axis of libration changing with time). The discrete scatterer proved to be the crater Tycho.

In many respects Tycho is well placed to be detected in observations such as these. It is at a range where the "quasi-specular" component contributes little to the echo, and is not near the edge of the spectrum where the resolution becomes poor due to the increased area in each cell (fig. 4). If Tycho were nearer the center of the Moon, it is doubtful if the range resolution afforded by the 0.5-msec pulses employed by Pettengill and Henry [1962a] would have been adequate to resolve it. These considerations partly account for why only Tycho was identified as an anomalous scatterer in this early work.

In view of the fact that the cells in Pettengill and Henry's "map" were of comparable size to the area occupied by Tycho, it is probable that the crater is actually about 10 times a better reflector than an equal area in its environs. This remarkable result is made all the more remarkable by the fact that it is equally bright with respect to its surroundings for the polarized and depolarized signals. This latter observation precludes any explanation based upon large flat facets normal to the line of sight in the vicinity of Tycho, since these would not be expected to depolarize.

If the surface material in the vicinity of Tycho were solid rock, exposed perhaps because there have been no subsequent impacts which could have covered it with rubble, or because any natural erosion processes have not been operating for a comparable length of time as elsewhere on the surface, then part of the anomaly can be accounted for by the increased reflection coefficient. It also seems reasonable to believe that the extreme roughness associated with fracturing (brecciation) caused by the original meteoric impact is still preserved and visible to the radar. (A thin layer of material overlying the rock could account for the optical behavior without influencing the radar scattering.) Thus the enhanced reflectivity may be explained as a combination of denser and rougher material in and around the crater as compared to the older unperturbed surroundings. Since only ~ 8 percent of the surface is thought to be rough (sec. 7) at this frequency, a 10-fold increase in reflectivity can just be obtained by assuming a localized region which is nearly a perfect Lambert scatterer. If, in addition, it is assumed that the surface reflection coefficient is higher (due to the increased density), then proportionally less roughness need be involved.

Shorthill [1962] has observed that virtually all the rayed craters have anomalous thermal properties at infrared. During eclipses or the waning cycle of the Moon, they cool less rapidly than their surroundings. The reverse is true during the waxing phase. This behavior can be attributed to the absence in these recent craters of an appreciable dust layer which overlies most of the remainder of the surface. The extent to which this effect is observed seems to bear a direct relation with the estimated age of the craters concerned (Tycho being the most conspicuous example). It is tempting to suppose that these same craters are also anomalous radar reflectors. Work presently underway to test this hypothesis, at the Arecibo Ionospheric Observatory, has shown that most of the rayed craters are indeed anomalously bright scatterers [Pettengill, private communication]. In this work unambiguous maps of regions of the lunar surface are obtained by using a pencil beam which discriminates against one of the pair of cells having the same range and Doppler coordinates.

The extraordinary reflectivity of these objects compared to their surroundings supports the view advanced earlier that most of the surface must be relatively smooth and covered to a very considerable depth (perhaps meters) with material that is broken and porous and no more dense than sand.

10. Summary

10.1. Distance Measurements

Accurate range measurements have been reported only by the group working at the Naval Research Laboratory [Yaplee et al., 1959]. Their most recent value for the mean center-to-center distance between the Earth and the Moon is $384{,}400.2 \pm 1.1$ km and is based upon a value for the Earth's radius of 6,378,170 m which seemed most consistent with the observed diurnal variation in range.

10.2. Cross-Section Measurements

The absolute cross section of the Moon has been determined over a wide range of wavelengths to a precision in most cases of ± 3 dB. Unfortunately,

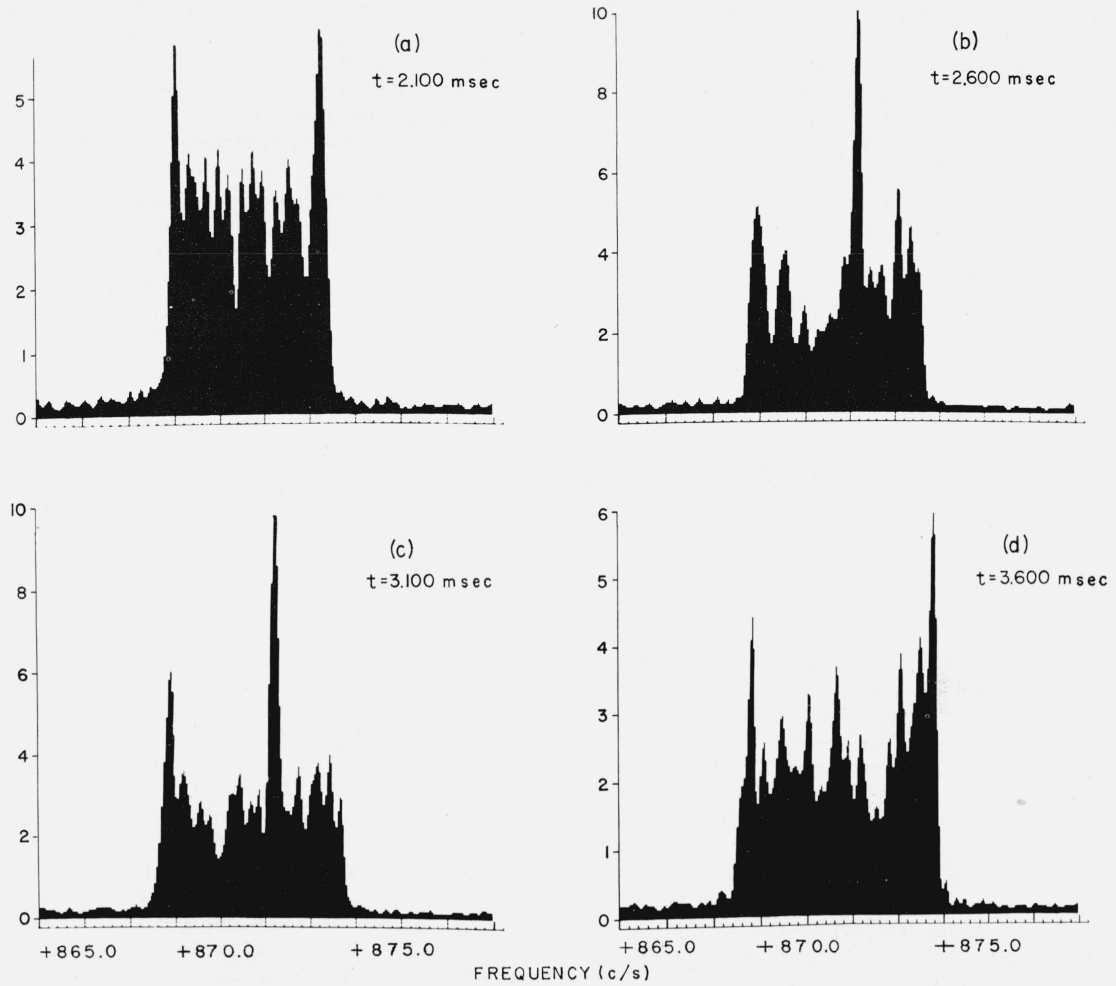

FIGURE 20. *Lunar echo power spectra at four intervals of range, taken 19 hr 00 min 19 sec UT, June 20, 1961.*

The central peaks in (b) and (c) correspond to the position of the crater Tycho. Peaks at the extremes of the spectra result from the large common area of the intersecting range and Doppler contours (fig. 4) and probably do not represent individual surface features.

this uncertainty is too large to permit any certain conclusions to be drawn concerning the wavelength dependence in the cross section. The observations suggest that the cross section remains constant at about 7 percent of the projected area of the Moon's disk at wavelengths in the range 1 cm to 1 m, and perhaps rises to 10 percent or higher at wavelengths in the range 1–10 m. It is possible that the wavelength independence in the range 1–100 cm arises as a consequence of two opposing effects. If the surface is broken and porous and has an average density that increases with depth, then the field penetration will be greatest at long wavelengths. At short wavelengths the waves penetrate only a short distance and encounter a low reflection coefficient. However, the backscatter gain is high because the surface is rough. As the wavelength is increased G_m decreases, but this is offset by an increase in the reflection coefficient $\bar{\rho}$. Eventually (at about 1-m wavelength) the rough elements on the surface contribute little to the total power, and hence the gain remains constant for all longer wavelengths.[7]

10.3. Angular Scattering Observations

Short-pulse observations can be used to explore the angular dependence in the scattering of radio waves by the lunar surface. Useful measurements have been made at wavelengths of 1130, 68, 23, 10 and 3.6 cm. The angular dependence has also been investigated at 8.6 mm, though here the angular resolution afforded by a narrow pencil-beam antenna was employed. At all six wavelengths, it appears that part of the echo arises from a highlight located at the center of the Moon's visible disk. A second component

[7] See note added in proof.

comes almost equally from the remaining parts of the surface. The division of power in the two components changes markedly as the wavelength is reduced. At 68 cm wavelength, 80 percent of the power is returned from the highlight, but at 8.6 mm only 15 percent can be associated with this component. The angular power spectrum $\bar{P}(\phi)$ observed for the power from the highlight also changes with wavelength indicating that the rms slope of the surface increases as the wavelength is reduced.

These observations have been interpreted as indicating that there is a wide range of structure sizes on the Moon. Also, it appears that as the scale size is reduced, the amount observable structure increases. Daniels [1961] has likened this to the appearance of electrical noise which has been passed through a low-pass filter having an exponential characteristic. On top of the long-wave undulations are smaller-scale fluctuations, and overlying these are yet others of smaller scale, and so on. At 68-cm wavelength, only about 8 percent of the surface appears to be covered with structure of the order of the wavelength in size; the remainder appears largely smooth and undulating with average slopes of the order of 1 in 6. At 3.6 cm approximately 14 percent of the surface appears rough, yet at 8.6 mm, perhaps 70 percent appears to be covered with structure comparable to the wavelength in size. These numbers are less reliable than the corresponding value at 68 cm, but if taken at face value suggest a remarkable increase in rough structure as one approaches 1-cm wavelength. That is, there must be a large amount of structure with a scale size of the order of 0.5 mm or 0.25 mm. It may be significant that this is about the value of the depth of the dust layer required to explain the infrared eclipse measurements [Pettit, 1961].

10.4. Dielectric Constant

The cross-section measurements yield the product of the reflection coefficient ρ_0 and the backscatter gain of the surface g. Hagfors [1964] has shown that for a smooth undulating surface where the rms slope $\sqrt{2}\alpha$ is small and no shadowing takes place, g has a value of the order of $1+\alpha^2$. The gain, g, to be associated with the diffuse component is less easily arrived at. For the want of a better approach, Evans and Pettengill [1963c] assumed that ρ_0 in (8) is the same as $\bar{\rho}$ in (10) for the diffuse component, and hence were able to attribute to the diffuse component the known gain of a Lambert sphere (8/3). On this basis, it has been possible to derive a reflection coefficient ρ which varies from 0.065 at $\lambda=68$ cm to 0.035 at $\lambda=8.6$ mm. The corresponding values of dielectric constant range from $k=2.79$ down to $k=2.13$. In view of the greater experimental difficulties together with the doubtful validity of the assumptions at 8.6-mm wavelength, this apparent wavelength dependence should be accepted with caution. If real, it may be caused by the finite conductivity of the material [i.e., $s \neq 0$ in (6)] or by inhomogeneity in the surface layers—the density perhaps increasing with depth. These values are larger than the values obtained radiometrically and this appears to be caused by the fact that part of the signal is neglected from the uppermost interface and part from the material. The packing factor for the uppermost material is extremely small in the range 10 to 30 percent.

10.5. Discrete Scatterers

So far we have been concerned with the statistical properties of the surface and have, in fact, made the assumption that the surface elements resolvable by radar have the same characteristics. This is not strictly true and by employing a coherent-pulse radar, it has been possible to resolve smaller regions of the lunar surface and observe that there is at least one type of anomalous reflector—the rayed craters like Tycho. Doubtless many other anomalies exist, and much attention in the next years will probably be focused on determining the location and characteristics of these.

10.6. Future Observations

Almost in all the areas described, new observational material is urgently required which is more accurate than that available at present. Thus useful measurements can be made at any wavelength simply by determining the cross section to better than ± 1 dB. The angular-scattering law changes so rapidly with wavelength that new observations at almost any wavelength would be welcome. To be really useful, however, they should have a resolution comparable with the measurements described here (i.e., 30 μsec or better). Determinations of the angular-scattering law with a resolution approaching 1 μsec are needed at all wavelengths in the first 30 to 50 μsec of the return. Finally, more attention should be devoted to the polarization properties of the surface. These could provide more information concerning the small-scale structure and perhaps the depth of the tenuous dust layer on the surface.

Note added in proof: The successful Ranger flights provided a large amount of information concerning the lunar surface on a scale comparable to that which governs the radio reflection properties [Heacock et al., 1965].[8] This showed that the lunar surface is indeed largely smooth and undulating as had been predicted, but few objects could be found with small radii of curvature which would be responsible for the diffuse component of the radio echoes. It would be possible for the waves to penetrate an upper layer of low density material, and be scattered from beneath. Accordingly, it was suggested that perhaps the rough structure responsible for the diffuse echoes lies under the visible surface. Experiments to test this hypothesis have recently been conducted by Hagfors et al., [1965] at Millstone Hill radar.[5]

If we suppose for the moment that the diffuse component of the echoes consists wholly of reflections from within the medium, then the strength of the echo will depend upon (a) the transmission coefficient into the surface, (b) the reflection coefficient within the medium, and (c) the transmission coefficient out of the surface. Of course (a) and (c) are the same provided the polarization is maintained unchanged. It seems that for large angles of incidence ϕ the reflec-

[8] Heacock, R. L., G. P. Kuiper, E. M. Shoemaker, H. C. Urey, and A. E. Whitaker (1965), Ranger VII Experimenter's analyses and interpretations, Tech. Rep. 32-700, Jet Propulsion Lab., Pasadena, Calif.

tion from within the surface will chiefly be from small scale structure and hence the reflection coefficient will be independent of the incident plane of polarization. Thus the intensity of the echo power from an isolated region of the lunar surface removed from the center of the disk should vary with the plane of the incident polarization, in a way which depends only upon the square of the transmission coefficient. For the case when the electric field lies in the local plane of incidence the transmission coefficient $T_{||}=(4\ k\ \cos\phi\sqrt{k-\sin^2\phi})/(k\ \cos\phi+\sqrt{k-\sin^2\phi})^2$ where k is the dielectric constant of the material, and for the field across the local plane of incidence $T_{\perp}=(4\cos\phi\sqrt{k-\sin^2\phi})/(\cos\phi+\sqrt{k-\sin^2\phi})^2$. The ratio $T_{\perp}/T_{||}$ varies with the angle of incidence ϕ is shown in figure 21. At $\phi=0$, $T_{\perp}T_{||}=1.0$ and for $\phi=90°$, $T_{\perp}/T_{||}=1/k$.

Regions of the Moon may be studied separately by employing range-Doppler mapping described in sec. 9. Let us consider only the echoes reflected from a strip of surface lying along the apparent axis of rotation (fig. 4), and suppose that this strip is illuminated first with a wave in which the electric field is parallel to the axis of rotation (case A) and then with a wave perpendicular to this axis (case B). In case A the echo power *in the diffuse region* will depend upon $(T_{||})^2$ and in the case B on $(T_{\perp})^2$ if the layer hypothesis is correct. In the experiment conducted by Hagfors et al. [1965] the Millstone Hill radar was employed at 23 cm wavelength.[5] The beamwidth is slightly larger than the angular diameter of the Moon so that the whole Moon was illuminated. The transmitted polarization was right circular, and this may be thought of as equivalent to transmitting orthogonal linear components with a phase shift of one quarter wavelength. On reception two orthogonal linear components were obtained whose orientation could be controlled at will. During the course of the experiment adjustments were made to maintain one of the linears alined along the apparent axis of rotation (libration axis), computed as a function of time in advance of the observations. The effect of Faraday rotation was determined to be small so that it could be ignored. The signals corresponding to the two linear components are amplified separately and coherently processed over a frequency range of ± 18 cps with a resolution of 2 cps. Spectra obtained at various delays with respect to the leading edge echo are shown in figure 22. The areas under the two spectra obtained at each delay were adjusted to be the same in order to remove any differences in the gains of the two receivers (or noncircularity of the transmitted wave). This was justified since the *total* power reflected from any range ring should be independent of the polarization of the wave. It can be seen in figure 22 that, as expected, component A is stronger than component B at the center of each spectrum. At the limbs of each spectrum (marked L) the orientation between the field and the surface is reversed and hence component B is now stronger than A. The points marked C have a value of 0.707 L and represent the points where the two components should be equally strong. The peak at +4 cps in the plot at a range of 4.48 msec is due to the crater Tycho, and exhibits no difference in the intensity of the two components. Presumably Tycho is not covered by a layer of light material, and this is in accord with conclusions reached in sec. 9 from the anomalously strong reflections obtained from this crater.

By taking the square root of the ratio of the powers at the center frequency Hagfors et al. [1965] obtained the experimental points shown in figure 21 for the ratio of the transmission coefficients. These points indicate that the upper surface has a dielectric constant of 1.8. If substantial parts of the lunar surface are not covered by this layer, or if some of the echo power at these delays is reflected from the top of this layer then the points in figure 21 will have been displaced upwards. It follows that a value $k=1.8$ is a lower limit. It is interesting and probably quite significant that this value corresponds very closely to the ones derived from radiometric observations of the polarization of the thermal emission from the lunar surface [Soboleva, 1962; Heiles and Drake, 1963] and other values inferred from passive observations [Troitsky, 1962; Salomonovich and Losovsky, 1962; and Krotikov and Troitsky, 1962]. All these values were found to lie in the range 1.5 to 2.0, and hence disagree with the radar value (2.6 to 2.8) derived earlier (in sec. 7).

Let us suppose that the lunar surface consists of two layers. The upper one is irregular in depth, largely smooth, and has a dielectric constant of 1.8. The lower one is somewhat denser and more irregular. Possibly also there may be irregularities in density within the upper layer which contribute to the backscattered power. The radiometric determinations of the dielectric constant based on the polarization of the thermal emission can be brought into line with

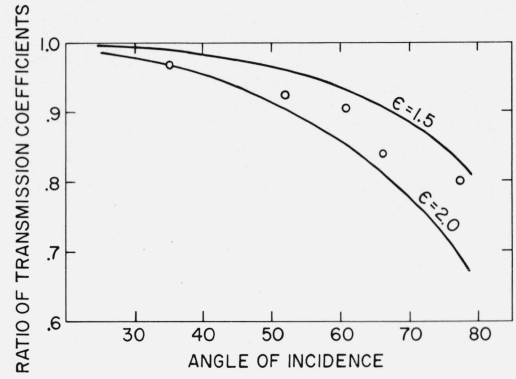

FIGURE 21. *The ratio between the transmission coefficients* $T_{\perp}$ *and* $T_{||}$ *obtained from equations given in the text for two values of the dielectric constant.*

The experimental points for the Moon were derived by Hagsfors et al. [1965] from the results presented in fig. 22.

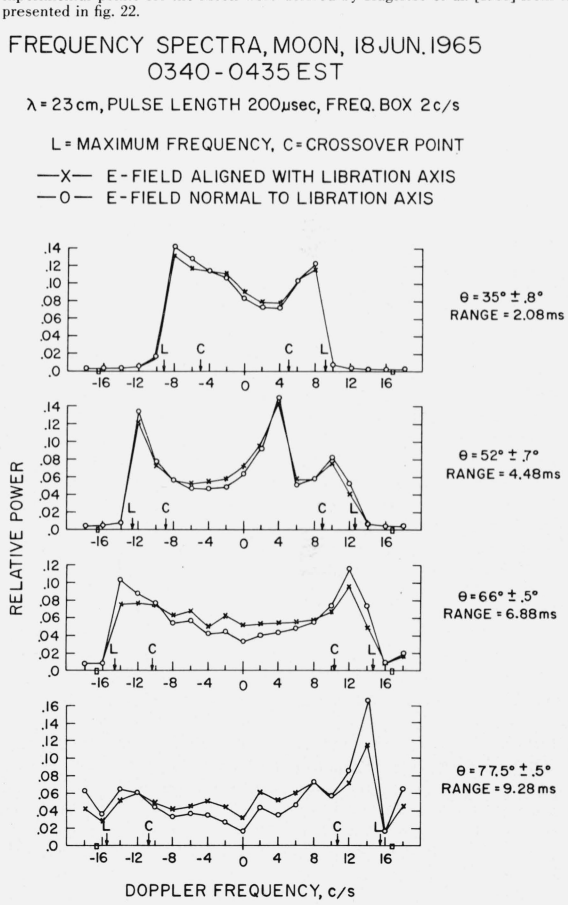

FIGURE 22. *Radio-frequency power spectra obtained by Hagfors et al. [1965] at various values of delay with respect to the center of the Moon.*

The two spectra obtained at each range are for linearly polarized waves parallel and at right angles to the apparent axis of libration. The systematic differences in the curves are due to the difference between the transmission coefficients (fig. 21) for the two directions.

this naive two layer model. Calculations show that near grazing angles of incidence the polarization of the emission will practically entirely be determined by the top layer. It therefore appears that a two layer model of the lunar surface of the type suggested provides a rather self-consistent explanation of several different types of observations made of the Moon by radio waves.

In order to reconcile the observed reflection coefficient at normal incidence (6%) with that expected for a homogeneous layer having

a dielectric constant $k = 1.8$ (i.e., 3%) it is necessary to have a base layer with a dielectric constant $k = 4.5$ to 5. As to the depth of the layer one can only say that it must be irregular and greater than 23 cm (i.e., the wavelength employed in these observations). If the depth is less than say 1 to 2 meters, one would be able to account for the increase in cross section observed by Davis and Rohlfs [1964] (see fig. 2), since a thin layer would be unimportant at decameter wavelengths. However as noted earlier these long wave measurements are extremely difficult to perform reliably and perhaps not too much importance should be attached to this possible upper limit.

In view of the fact that at normal incidence some 60 percent of the echo power is reflected from within the surface, we are obliged to ask, what if any, is the meaning of the distributions and rms values of the surface slopes obtained in sec 4? The answer is that these cannot apply to the uppermost layer, but to some hypothetical surface lying within that layer. For a two layer model this hypothetical surface would roughly lie midway between the two boundaries and have characteristics roughly comparable to the sum of the two layers. It follows that since the hypothetical surface is largely smooth and undulating neither boundary can be particularly rough. In our present interpretation we have ascribed the small scale roughness entirely to the base layer, but this may be improper. A variety of models can be invented which would match the results. For example, density irregularities within the upper layer (e.g., boulders) might be responsible for the diffuse component. A value of the dielectric constant of 1.8 implies that the material must have a porosity roughly in the range 70 to 90 percent if the material in bulk is not very dissimilar from terrestrial rocks.

11. References

Beckmann, P. (1964a), Scattering by composite rough surfaces, Dept. of Elec. Engr., Univ. of Colorado, Report No. 4.

Beckmann, P. (1964b), Radar backscatter from the surface of the moon, Dept. of Elec. Engr., Univ. of Colorado, Report No. 5.

Blevis, B. C., and J. H. Chapman (1960), Characteristics of 488 megacycles per second radio signals reflected from the moon, J. Res. NBS **64D,** (Radio Prop.) No. 4, 331–334.

Bowhill, S. A. (1957), Ionospheric irregularities causing random fading of very low frequencies, J. Atmospheric Terrest. Phys. **11,** 91–101.

Bramley, E. N. (1962), A Note on the theory of moon echoes, Proc. Phys. Soc. (London) **80,** 1128–1132.

Brown, W. E. (1960), A lunar and planetary echo theory, J. Geophys. Res. **65,** 3087–3095.

Browne, I. C., J. V. Evans, J. K. Hargreaves, and W. A. S. Murray (1956), Radio echoes from the moon, Proc. Phys. Soc. (London) **B69,** 901–920.

Brunschwig, M., W. E. Fensler, E. Knott, A. Olte, K. M. Siegel, T. J. Ahrens, J. R. Dunn, F. B. Gerhard, Jr., S. Katz, and J. L. Rosenholtz (1960), Estimation of the physical constants of the lunar surface, Univ. of Mich. Report 3544–1–F.

Daniels, F. B. (1961), A theory of radar reflection from the moon and planets, J. Geophys. Res. **66,** 1781–1788.

Daniels, F. B. (1962), Author's comments on the preceding discussion, J. Geophys. Res. **67,** 895.

Daniels, F. B. (1963a), Radar determination of the root mean square slope of the lunar surface, J. Geophys. Res. **68,** 449–453.

Daniels, F. B. (1963b), Radar determination of lunar slopes: correction for the diffuse component, J. Geophys. Res. **68,** 2864–2865.

Davis, J. R., and D. C. Rohlfs (1964), Lunar radio-reflection properties at decameter wavelengths, J. Geophys. Res. **69,** 3257–3262.

DeWitt, J. H., Jr., and E. K. Stodola (1949), Detection of radio signals reflected from the moon, Proc. IRE **37,** 229–242.

Dollfus, A. (1962), The polarization of moonlight, Physics and Astronomy of the Moon, ed. Z. Kopal, ch. 5 (Academic Press, London).

Edison, A. R., R. K. Moore, and B. D. Warner (1959), Radar return at near-vertical incidence—summary report, Univ. of New Mexico Tech. Rept. EE–24.

Evans. J. V. (1957), The scattering of radiowaves by the moon, Proc. Phys. Soc. (London) **B70,** 1105–1112

Evans, J. V. (1962a), Radio echo studies of the moon, Physics and Astronomy of the Moon, ed. Z. Kopal, ch. 12 (Academic Press, London).

Evans, J. V. (1962b), Radio echo observations of the moon at 3.6 cm wavelength, MIT Lincoln Lab. Tech. Rept. 256, ASTIA No. DDC 274669.

Evans, J. V. (1962c), Radio echo observations of the moon at 68 cm wavelength, MIT Lincoln Lab Tech. Rept. 272, ASTIA No. DDC 291102.

Evans, J. V., S. Evans, and J. H. Thomson (1959), The rapid fading of moon echoes at 100 Mc/s, Paris Symposium on Radio Astronomy, ed. R. N. Bracewell, p. 8 (Stanford Univ. Press, Stanford, Calif).

Evans, J. V., and T. Hagfors (1964), On the interpretation of radar reflections from the moon, Icarus **3,** 151–160.

Evans, J. V., and T. Hagfors (1965), The scattering of the moon at 23 cm wavelength, unpublished.

Evans, J. V., and R. P. Ingalls (1962), Radio echo studies of the moon at 7.84 meter wavelength, MIT Lincoln Lab Tech. Rept. 288, ASTIA No. DDC 294008.

Evans, J. V., and G. H. Pettengill (1963a), The radar cross section of the moon, J. Geophys. Res. **68,** 5098–5099.

Evans, J. V., and G. H. Pettengill (1963b), The scattering properties of the lunar surface at radio wavelengths, The Solar System, vol. **4,** The Moon, Meteorites and Comets, ed. G. P. Kuiper and B. M. Middlehurst, ch. 5 (Univ. of Chicago Press, Chicago).

Evans, J. V., and G. H. Pettengill (1963c), The scattering behavior of the moon at wavelengths of 3.6, 68 and 784 centimeters, J. Geophys. Res. **68,** 423–447.

Fricker, S. J., R. P. Ingalls, W. C. Mason, M. L. Stone, and D. W. Swift (1958), Characteristics of moon reflected UHF signals, MIT Lincoln Lab Tech. Rept. 187, ASTIA No. DDC 204519.

Fricker, S. J., R. P. Ingalls, W. C. Mason, M. L. Stone, and D. W. Swift (1960), Computation and measurement of the fading rate of moon-reflected UHF signals, J. Res. NBS **64D,** (Radio Prop.), No. 5, 455–465.

Fung, A. K., and R. K. Moore (1964), Effects of structure size on moon and earth radar returns at various angles, J. Geophys. Res. **69,** 1075–1081.

Gold T. (Jan. 1964), Presented to the MIT Compass Seminar, Cambridge, Mass.

Grant, C. R., and B. S. Yaplee (1957), Backscattering from water and land at centimeter and millimeter wavelengths, Proc. IRE **45,** 976–982.

Grieg, D. D., S. Metzger, and R. Waer (1948), Considerations of moon-relay communication, Proc. IRE **36,** 652–663.

Hagfors, T. (1961), Some properties of radio waves reflected from the moon and their relation to the lunar surface, J. Geophys. Res. **66,** 777–785.

Hagfors, T. (1964), Backscattering from an undulating surface with applications to radar returns from the moon, J. Geophys. Res. **69,** 3779–3784.

Hagfors, T. (1965), The relationship of the geometric optics and the autocorrelation approaches to the analysis of lunar and planetary radar echoes, presented at the International URSI Meeting on Planetary Surfaces and Atmospheres, Arecibo, Puerto Rico.

Hapke, B. W., and H. Van Horn (1963), Photometric studies of complex surfaces with applications to the moon, J. Geophys. Res. **68,** 4545–4570.

Hargreaves, J. K. (1959), Radio observations of the lunar surface, Proc. Phys. Soc. (London) **B73,** 536–537.

Hayre, H. S., and R. K. Moore (1961), Theoretical scattering coefficient for near vertical incidence from contour maps, J. Res. NBS **65D** (Radio Prop.), 427–432.

Heiles, C. E., and F. D. Drake (1963), The polarization and intensity of thermal radiation from a planetary surface, Icarus **2,** 281–292.

Hey, J. S., and V. A. Hughes (1959), Radar observations of the moon at 10 cm wavelength, Paris Symposium on Radio Astronomy, ed. R. N. Bracewell, p. 13 (Stanford Univ. Press, Stanford, Calif.).

Hughes, V. A. (1961), Radio wave scattering from the lunar surface, Proc. Phys. Soc. (London) **78,** 988–997.

Hughes, V. A. (1962a), Diffraction theory applied to radio wave scattering from the lunar surface, Proc. Phys. Soc. (London) **80,** 1117–1127.

Hughes, V. A. (1962b), Discussion of paper by Daniels "A theory of radar reflections from the moon and planets", J. Geophys. Res. **67,** 892–894.

Kerr, F. J., and C. A. Shain (1951), Moon echoes and transmission through the ionosphere, Proc. IRE **39,** 230–242.

Krotikov, V. D., and V. S. Troitsky (1962), The emissivity of the moon at centimeter wavelengths, Astron. Zh. (USSR) **39,** 1089–1093.

Leadabrand, R. L., R. B. Dyce, A. Fredriksen, R. I. Presnell, and R. C. Barthle (1960), Evidence that the moon is a rough scatterer at radio frequencies, J. Geophys. Res. **65,** 3071–3078.

Lynn, V. L., M. D. Sohigian, and E. A. Crocker (1963), Radar observations of the moon at 8.6 mm wavelength, MIT Lincoln Lab. Tech. Rept. 331, ASTIA No. DDC 426207 (1963). See also, J. Geophys. Res. **69**, 781–783 (1964).
Markov, A. V. (1948), Brightness distribution over the lunar disk at full moon, Astron. Zh. (USSR) **25**, 172–179.
Muhleman, D. O. (1964), Radar scattering from Venus and the moon, Astron. J. **69**, 34–41.
Norton, K. A. and A. C. Omberg (1947), The maximum radar set, Proc. IRE **35**, 4–24.
Pettengill, G. H. (1960), Measurements of lunar reflectivity using the Millstone radar, Proc. IRE **48**, 933–934.
Pettengill, G. H., and J. C. Henry (1962a), Radio measurements of the lunar surface, The Moon, IAU Symposium 14, ed. Z. Kopal and Z. K. Mikailov, 519–525 (Academic Press, London).
Pettengill, G. H., and J. C. Henry (1962b), Enhancement of radar reflectivity associated with the lunar crater Tycho, J. Geophys. Res. **67**, 4881–4885.
Pettit, E. (1961), Planetary temperature measurements, The Solar System, vol. **3**, Planets and Satellites, ed. G. P. Kuiper and B. M. Middlehurst, ch. 10 (Univ. of Chicago Press, Chicago).
Rea, D. G., N. Hetherington, and R. Mifflin (1964), The analysis of radar echoes from the moon, J. Geophys. Res. **69**, 5217–5223.
Salomonovich, A. E., and B. Y. Losovsky (1962), Radio brightness distribution of the lunar disk at 0.8 cm, Astron. Zh. (USSR) **39**, 1074–1082.
Senior, T. B. A., and K. M. Siegel (1959), Radar reflection characteristics of the moon, Paris Symposium on Radio Astronomy, ed. R. N. Bracewell, p. 29 (Stanford Univ. Press, Stanford, Calif.).
Senior, T. B. A., and K. M. Siegel (1960), A theory of radar scattering by the moon, J. Res. NBS **64D** (Radio Prop.), No. 3, 217–228.
Shorthill, R. W. (1962), Measurements of lunar temperature variations during an eclipse and throughout a lunation, Boeing Report D.1. 82–0196.
Soboleva, N. S. (1962), Measurement of the polarization of lunar radio emission on a wavelength of 3.2 cm, Astron. Zh. (USSR) **39**, 1124–1126.
Trexler, J. H. (1958), Lunar radio echoes, Proc. IRE **46**, 286–292.
Troitsky, V. S. (1962), Radio emission of the moon, its physical state and the nature of its surface, The Moon, IAU Symposium 14, ed. Z. Kopal and Z. K. Mikhailov, p. 475 (Academic Press, London).
Twersky, V. (1962), On scattering of waves by random distributions, II. Two space scatterer formalism, J. Math. Phys. **3**, 724–734.
Victor, W. K., R. Stevens, and S. W. Golomb (1961), Radar exploration of Venus, Jet Propulsion Lab Tech. Rept. 32–132.
Winter, D. F. (1962), A theory of radar reflections from a rough moon, J. Res. NBS **66D** (Radio Prop.), No. 3, 215–226.
Yaplee, B. S., R. H. Bruton, K. J. Craig, and N. G. Roman (1958), Radar echoes from the moon at a wavelength of 10 cm, Proc. IRE **46**, 293–297.
Yaplee, B. S., N. G. Roman, K. J. Craig, and T. F. Scanlon (1959), A lunar radar study at 10 cm wavelength, Paris Symposium on Radio Astronomy, ed. R. N. Bracewell, p. 19 (Stanford Univ. Press, Stanford, Calif.).
Yaplee, B. S., S. H. Knowles, A. Shapiro, K. J. Craig, and D. Brouwer (1964), The mean distance to the moon as determined by radar, Naval Research Lab Rept. 6134.

(69D12–618)

Decameter-Wave Radar Studies of the Lunar Surface

J. R. Davis, D. C. Rohlfs, G. A. Skaggs, and J. W. Joss [1]

Radar Division, U.S. Naval Research Laboratory, Washington, D.C.

An extended series of decameter-wave measurements of the total radar cross section of the Moon has corroborated a previous suggestion that this parameter has a substantially larger value in the decameter region than at shorter wavelengths. Examples are given of the ionospheric effects which require decameter-wave measurements conducted over a transionospheric path to be regarded with caution. A beginning study of possible discrete scattering centers located in regions toward the limb of the Moon is described.

1. Introduction

The U.S. Naval Research Laboratory, as part of a continuing program of research in radio propagation and radar techniques, has conducted a high-frequency (HF) radar study of the Moon and transionospheric propagation for the past 3½ years. Measurements of Moon-reflected radar signals at wavelengths between 11 and 22 m have been made on a regular basis during this period with the use of NRL's high-power HF transmitting facility. As is often the case with decameter-wave radio undertakings, however, the pattern of the large broadside array which has been used for this series of measurements has imposed severe restrictions on the operating schedule. Observations have been possible only for periods of approximately 1½ hr immediately after moonrise on the few days each month when the Moon's delination exceeds 15° North. Due to the ionospheric phenomena which affect decameter-wave radio signals, useful observations have been possible only during periods well after ionospheric sunset, as well.

In brief, the NRL high-power HF transmitting facility has been utilized in a monostatic, pulsed mode for this study, providing pulses of approximately 250 μsec in length at pulse repetition frequencies of 5⅝ pulses per second and harmonically related multiples of that rate. Observations have centered largely upon measurements of two principal characteristics of the Moon as a decameter-wave radar target:

(a) Its total radar cross section, and

(b) its properties as a distributed scatterer.

An earlier series of measurements conducted with this facility [Davis and Rohlfs, 1964] has suggested that both of these parameters display somewhat different character at decameter wavelengths than in the meter and centimeter regions. In particular, the Moon's total radar cross section has been measured to be substantially *larger* at decameter wavelengths than at shorter wavelengths, and the relative contribution to the total scattered energy by areas beyond the Moon's central, specularly reflecting region has been measured to be distinctly *less* in the decameter region than at shorter wavelengths. This behavior has led to the suggestion than the Moon, apparently a perfectly rough or uniformly bright reflector at optical wave-

[1] RCA Service Company.